OPEN

Molecular Signaling and Dysfunction of the Human Reactive Enteric Glial Cell Phenotype: Implications for GI Infection, IBD, POI, Neurological, Motility, and GI Disorders

Andromeda Liñán-Rico, PhD, Fabio Turco, PhD,† Fernando Ochoa-Cortes, PhD,* Alan Harzman, MD,‡ Bradley J. Needleman, MD,‡ Razvan Arsenescu, MD,§ Mahmoud Abdel-Rasoul, MS, MPH,‖ Paolo Fadda, PhD,¶ Iveta Grants, BSc,* Emmett Whitaker, MD,** Rosario Cuomo, PhD,† and Fievos L. Christofi, PhD**

Background: Clinical observations or animal studies implicate enteric glial cells in motility disorders, irritable bowel syndrome, inflammatory bowel disease, gastrointestinal (GI) infections, postoperative ileus, and slow transit constipation. Mechanisms underlying glial responses to inflammation in human GI tract are not understood. Our goal was to identify the "reactive human enteric glial cell (rhEGC) phenotype" induced by inflammation, and probe its functional relevance.

Methods: Human enteric glial cells in culture from 15 GI-surgical specimens were used to study gene expression, Ca^{2+}, and purinergic signaling by Ca^{2+}/fluo-4 imaging and mechanosensitivity. A nanostring panel of 107 genes was designed as a read out of inflammation, transcription, purinergic signaling, vesicular transport protein, channel, antioxidant, and other pathways. A 24-hour treatment with lipopolysaccharide (200 μg/mL) and interferon-γ (10 μg/mL) was used to induce inflammation and study molecular signaling, flow-dependent Ca^{2+} responses from 3 mL/min to 10 mL/min, adenosine triphosphate (ATP) release, and ATP responses.

Results: Treatment induced a "rhEGC phenotype" and caused up-regulation in messenger RNA transcripts of 58% of 107 genes analyzed. Regulated genes included inflammatory genes (54%/IP10; IFN-γ; CxCl2; CCL3; CCL2; C3; s100B; IL-1β; IL-2R; TNF-α; IL-4; IL-6; IL-8; IL-10; IL-12A; IL-17A; IL-22; and IL-33), purine-genes (52%/AdoR2A; AdoR2B; P2RY1; P2RY2; P2RY6; P2RX3; P2RX7; AMPD3; ENTPD2; ENTPD3; and NADSYN1), channels (40%/Panx1; CHRNA7; TRPV1; and TRPA1), vesicular transporters (SYT1, SYT2, SNAP25, and SYP), transcription factors (relA/relB, SOCS3, STAT3, GATA_3, and FOXP3), growth factors (IGFBP5 and GMCSF), antioxidant genes (SOD2 and HMOX1), and enzymes (NOS2; TPH2; and CASP3) ($P < 0.0001$). Treatment disrupted Ca^{2+} signaling, ATP, and mechanical/flow-dependent Ca^{2+} responses in human enteric glial cells. ATP release increased 5-fold and s100B decreased 33%.

Conclusions: The "rhEGC phenotype" is identified by a complex cascade of pro-inflammatory pathways leading to alterations of important molecular and functional signaling pathways (*Ca^{2+}, purinergic, and mechanosensory*) that could disrupt GI motility. Inflammation induced a "purinergic switch" from ATP to adenosine diphosphate/adenosine/uridine triphosphate signaling. Findings have implications for GI infection, inflammatory bowel disease, postoperative ileus, motility, and GI disorders.

(Inflamm Bowel Dis 2016;22:1812–1834)

Key Words: human enteric glial cells, bacterial lipopolysaccharide, purinergic signaling, mechanosensitivity, Ca^{2+} signaling, ATP, adenosine

"Glial cell excitability" is determined by changes in intracellular free Ca^{2+} signals. Emerging evidence suggests that enteric glial cell (EGC) Ca^{2+} signals modulate motility and transit.[1–3] Purinergic Ca^{2+} signaling is an important mechanism in glial cell physiology. Clinical observations and animal studies implicate EGC in enteric nervous system (ENS) and motility disorders associated with

Supplemental digital content is available for this article. Direct URL citations appear in the printed text and are provided in the HTML and PDF versions of this article on the journal's Web site (www.ibdjournal.org).

Received for publication January 14, 2016; Accepted February 3, 2016.

From the *Department of Anesthesiology, Wexner Medical Center, The Ohio State University, Columbus, Ohio; †Gastroenterological Unit, Department of Clinical and Experimental Medicine, "Federico II" University of Naples, Naples, Italy; ‡Department of Surgery, Wexner Medical Center, The Ohio State University, Columbus, Ohio; §Department of Internal Medicine, Wexner Medical Center, The Ohio State University, Columbus, Ohio; ‖Center for Biostatistics, Wexner Medical Center, The Ohio State University, Columbus, Ohio; ¶Comprehensive Cancer Center, The Ohio State University, Columbus, Ohio; and **Nationwide Children's Hospital, Department of Anesthesiology and Pain Medicine, Columbus, Ohio.

Author disclosures are available in the Acknowledgments.

Address correspondence to: Fievos L. Christofi, PhD, Department of Anesthesiology, The Wexner Medical Center, The Ohio State University, 226 Tzagournis Medical Research Facility, 420 West 12th Avenue, Columbus, OH 43210 (e-mail: fedias.christofi@osumc.edu).

DOI 10.1097/MIB.0000000000000854

Published online 13 July 2016.

slow transit constipation, irritable bowel syndrome, inflammatory bowel disease, postoperative ileus, (POI), gastrointestinal (GI) infections, and barrier-pathology.[4–6]

Several recent studies have provided new insights on our understanding of the pro-inflammatory mechanisms linked to the reactive human enteric glial cell (rhEGC) phenotype and its relevance as a therapeutic target for GI disorders. The study by Turco et al[7] was the first to show that enteroinvasive Escherichia coli interact with human enteric glial cells (hEGC), and the bacterial toxin lipopolysaccharide (LPS) acts via toll-like receptors 4 (TLR4) to stimulate production of nitric oxide (NO) through a RAGE/s100B/inducible nitric oxide synthase (iNOS)–dependent signaling pathway. Furthermore, hEGC can discriminate between beneficial and harmful bacteria for TLR4 activation (i.e., only enteroinvasive Escherichia coli can activate TLR4). The second study by Esposito et al[8] explored palmitoylethanolamide as a potential drug target for ulcerative colitis. It was shown to act by blocking inflammation in animals and humans by targeting the TLR4/s100B–dependent activation of peroxisome proliferator-activated receptors α in EGC to inhibit nuclear factor (NF)-kB–dependent inflammation. A third study in animals implicates the EGC in POI. POI, common in abdominal surgery, is associated with a significant risk of postoperative complications, and carries a heavy economic burden.[6] POI may involve interleukin (IL)-1 receptor signaling in EGC, and manipulations that block IL-1 signaling are protective against development of POI.[9] Therefore, a drug that can interfere with IL-1 signaling in glia is a potential therapeutic target.

An emerging concept is that intestinal inflammation associated with IBD or intestinal infection induces a "rhEGC phenotype" that could alter neural and motor behavior of the gut.[6] Knowledge about the rhEGC phenotype remains limited, and its functional consequences in glial networks are not known. To date, no systematic analysis of the impact of inflammation or infection has been done to identify the molecular and functional consequences in hEGC. To do this, and address this gap in knowledge, we designed a custom panel of 107 genes based on their association with intestinal inflammation and IBD to use as a readout for changes in gene expression profiles in response to bacterial LPS, in a model of hEGC cultures obtained from human surgical specimens. We anticipated that the molecular readout would reveal a significant component of the molecular signature profile of the rhEGC phenotype. Furthermore, we hypothesized that significant disruption of glial function and Ca^{2+} signaling would occur in response to bacterial lipopolysaccharide.

The hEGC culture model was shown to be a suitable model to study glial function.[10,11] Our recent study established that hEGC displays Ca^{2+} oscillations, Ca^{2+} waves, and dynamic changes in intracellular free Ca^{2+} levels in response to stimulation. Propagating Ca^{2+} waves within the glial network also occur in intact human ENS in situ.[6] Furthermore, it was shown that mechanical stimulation (MS) and purinergic signaling play key roles in the physiology of hEGC–they trigger Ca^{2+} oscillations and Ca^{2+} waves in hEGC. Multiple purinergic receptors and mechanisms operate in hEGC, including adenosine receptors, nucleotide ionotropic P2X channel receptors, and metabotropic P2Y receptors.[10–12] Purinergic signaling pathways are sensitive to inflammation and changes in purinergic gene expression is known to occur for receptors and enzymes in purinergic pathways in response to gut inflammation.[13] Therefore, molecular pathways for purine genes were a major component of our gene platform, as well as functional studies on purinergic and mechanosensory signaling. We tested the hypothesis that inflammation would cause significant alterations in these signaling pathways. Functional end points on the impact of inflammation on hEGC were Ca^{2+} signaling and handling, purinergic (adenosine triphosphate [ATP]) Ca^{2+} responses, ATP release, and mechanosensitivity; these responses are well characterized in cultures of hEGC.[11]

Our findings provided significant new insights into the molecular mechanisms and pathophysiology of the rhEGC phenotype. Inflammation has a profound influence on Ca^{2+} signaling, purinergic signaling, and mechanosensitivity in hEGC. Overall, bacterial LPS induction disrupts glial function and specifically, it alters mechanical-evoked/flow-dependent Ca^{2+} oscillations, ATP responses, release of ATP and s100β, and Ca^{2+} handling. Disruption of glial function is likely to disrupt ENS and motility. The 65 genes shown to be sensitive to transcriptional regulation by LPS induction represent new targets of investigation in GI infections, neurological and GI disorders, POI, and inflammatory diseases, and may lead to potential novel therapeutic strategies. Our study also identified multiple candidate gene targets for purinergic pipeline drugs. Pipeline purinergic drugs have shown efficacy in preclinical models of IBD, irritable bowel syndrome, and pain, and many are in clinical trials for chronic inflammatory diseases (rheumatoid arthritis/psoriasis/IBD), visceral pain, GI disorders, and Crohn's disease (CD) with some encouraging results.[13]

MATERIALS AND METHODS

Human Surgical Specimens

The institutional review board protocol is approved by the ethics committee of the College of Medicine, The Ohio State University. Informed consent was obtained to procure human surgical tissue from colon or small bowel from patients with polyps undergoing a colectomy (sigmoid colon) or patients undergoing Roux-en-Y bypass surgery (jejunum). Human EGCs in culture from 15 GI-surgical specimens were used to study gene expression, Ca^{2+} and purinergic signaling by Ca^{2+}/fluo-4 imaging, ATP release, and mechanosensitivity.

Human EGC Isolation from Human Surgical Specimens and Culture

Tissue collection was performed by the surgeon and immersed immediately in ice cold oxygenated Krebs solution and promptly transported to the research facilities within 15 minutes in coordination with the clinical pathology team. For isolating myenteric ganglia, tissue was pinned luminal side facing up under a stereoscopic microscope and the mucosa, submucosa,

and most of the circular muscle were dissected away using scissors, and then flipped over to remove longitudinal muscle by dissection. For isolating submucous ganglia, the muscle layers are first removed by dissection, the tissue is flipped over and mucosa layer is carefully dissected away from the submucous plexus. Myenteric or submucous plexus tissue was cut and enzymatically dissociated as described elsewhere[7] with modifications as follows: Tissue (0.3–0.5 cm^2 pieces) was dissociated in a mixture of protease/collagenase (1 mg/mL each in Hanks balanced salt solution) for 60 minutes at 37°C; Ganglia were removed from the enzymatic solution by spinning down (twice), and re-suspended in Hanks balanced salt solution (once) and a mixture of Dulbecco's modified Eagle's medium (DMEM)-F12, bovine serum albumin 0.1%, and DNase 50 μg/mL (once). Afterwards, ganglia in Hanks balanced salt solution/DMEM-F12 were transferred into a 100-mm culture dish and collected with a micropipette while visualized under a stereoscopic microscope and plated into wells of a 24-well culture plate and kept in DMEM-F12 (1:1) medium containing 10% fetal bovine serum (FBS) and a mixture of antibiotics (penicillin 100 U/mL, streptomycin 100 μg/mL, and amphotericin B 0.25 μg/mL) at 37°C in an atmosphere of 5% CO_2 and 95% humidity. After cells reach semiconfluence in 3 to 4 weeks (P1), hEGC were enriched and purified by eliminating/separating fibroblasts, smooth muscle, and other cells. EGC enrichment and purification was achieved by labeling the isolated cells with magnetic micro beads linked to antispecific antigen, D7-Fib, and passing them through a magnetic bead separation column following the manufacturer instructions (Miltenyi Biotec Inc., San Diego, CA). This purification protocol was performed twice (P2 and P3) to reach cell enrichment of up to 10,000-fold, and 20,000 cells were plated on glass coverslips precoated with laminin/P-D-Lys 20 μg/mL in 50-mm bottom glass #0 culture dishes for fluo-4/AM calcium imaging. Cultured hEGC were kept until confluent, and harvested for additional experiments (4–10 d). The day of the experiment, hEGC were stimulated as indicated. Parallel to this, cells at each passage were split and seeded on plastic 25-mm^2 culture flasks and used for study in passages 3 to passage 7.

Ca^{2+} Imaging

Feeding medium was removed and cells were incubated for 30 minutes at 37°C with 2 μM fluo-4/AM (Molecular Probes, Eugene, OR) in DMEM with no FBS. After removing this solution, it was replaced with DMEM without FBS, and incubated at 37°C for an additional 30 minutes. At the end of this incubation, cells were removed from the incubator and placed on the stage of an upright Nikon Eclipse FN1 microscope (Nikon, Tokyo, Japan) with a ×20-water immersion objective. Calcium changes were visualized with a high sensitivity and resolution ANDOR iXon Ultra 897 EMCCD camera (Andor, Belfast, United Kingdom) capable of 54 frames/s video recording. Cells were perfused with a peristaltic pump at 4 mL/min with oxygenated Krebs solution (mM: NaCl 120, KCl 6.0, $MgCl_2$ 1.2, NaH_2PO_4 1.35, $NaHCO_3$ 14.4, $CaCl_2$ 2.5, and glucose 12.7). A "solution inline heater" (Warner Instruments, Inc., Hamden, CT) was used to maintain the perfusion temperature at 36.5°C ± 0.5°C. Time-series analysis of $[Ca^{2+}]_i$ was done at 0.1 to 0.034-second intervals (10–29 frames/s). Calcium image analysis was performed with NIS Elements Advanced Research software (Nikon).

Custom-design of Nanostring Panel of 107 Genes

Table 1 is a list of the 107 genes included in our custom-designed panel of genes for nanostring analysis to identify a rhEGC phenotype. The panel includes important genes in IBDs (from animal and human studies).[6,13–17]

A nanostring panel of 107 genes was designed as a read out of inflammation (of 23 cytokines and chemokines), 7 transcription factors, 18 purinergic receptors (including adenosine, P2X and P2Y–families), 12 purinergic enzymes (for adenosine, nucleotide, and di-nucleotide metabolism), 6 vesicular transport proteins, 6 different cation channels (i.e., for K^+, Ca^{2+}, hemichannels, transient receptor potential, and nicotinic channel), other enzymes, and post-receptor signaling pathways (i.e., cAMP pathway, PKC pathway, superoxide dismutase 2 [SOD2], caspase3/apoptotic pathway, heme oxygenase pathway, nitric oxide synthase 2 [NOS2], other receptors and proteins [including tight-junction proteins, growth factors, glial proteins, retinol binding protein, cadherins, etc.]).

LPS Induction in hEGC

EGCs were grown in 12-well dishes (2×10^4 cells in each well) in DMEM supplemented with 10% FBS and 1% penicillin–streptomycin, until confluence was reached (7–10 d). Cell cultures were grown individually from 6 different patients and were used at passages 4 to 7 for molecular signaling, Ca^{2+} imaging and release studies. EGCs isolation was performed from jejunum myenteric plexus (MP) (2 patients), colon MP (3 patients), and colon submucous plexus (SMP) (1 patient).

To study the response of hEGCs to inflammatory mediators, cells were incubated 24 hours with LPS (from *Escherichia coli*, 200 μg/mL, Sigma-Aldrich, St. Louis, MO) and interferon-gamma (IFN-γ) 10 μg/mL, Fisher Scientific (Item #285 IF 100, RHIFN-G human IFN-γ) in 400 μL of DMEM with 10% FBS and 1% penicillin–streptomycin. For controls, the medium alone was used. Supernatants (300 μL) were collected and immediately frozen in liquid nitrogen for measurement of ATP or s100β release.

RNA Isolation

Cells were lysed in TRIZOL (Thermo Fisher Scientific, Waltham, MA) and frozen at −80°C. Total RNA isolation was performed using the TRIZOL method and after the separation of the aqueous and organic phases, a RNA cleanup and concentration kit (NORGEN Biotek Corp., Ontario, Canada) was used to purify and increase the concentration of the RNA. Gene expression analysis was conducted using the Nanostring nCounter Analysis System (Nanostring Technologies, Seattle, WA).

NanoString nCounter Gene Expression Assay

The RNA quality has been evaluated using Agilent RNA 6000 Nano Chip. NanoString nCounter technology is based on

TABLE 1. Gene Set for Nanostring Analysis in hEGC

No.	Symbol	Official Full Name	Source http://www.genenames.org/data/hgnc_data.php?hgnc_id=262
Inflammation			
1	CCL2	Chemokine (C-C motif) ligand 2	HGNC:10618
2	CCL3	Chemokine (C-C motif) ligand 3	HGNC:10627
3	IP10	Chemokine (C-X-C motif) ligand 10	HGNC:10637
4	Cxcl2	Chemokine (C-X-C motif) ligand 2	HGNC:4603
5	C3	Complement component 3	HGNC:1318
6	IFN-G	IFN-gamma	HGNC:5438
7	IL-1ra	Interleukin-1 receptor antagonist	HGNC:6000
8	IL-1b	Interleukin-1, beta	HGNC:5992
9	IL-10	Interleukin 10	HGNC:5962
10	IL-12 A	Interleukin 12A	HGNC:5969
11	IL-13	Interleukin 13	HGNC:5973
12	IL-17A	Interleukin 17A	HGNC:5981
13	IL-2R	Interleukin 2 receptor, α	HGNC:6008
14	IL-22	Interleukin 22	HGNC:14900
15	IL-23A	Interleukin 23, alpha subunit p19	HGNC:15488
16	IL-33	Interleukin 33	HGNC:16028
17	IL-4	Interleukin 4	HGNC:6014
18	IL-5	Interleukin 5	HGNC:6016
19	IL-6	Interleukin 6	HGNC:6018
20	IL-8	Interleukin 8	HGNC:6025
21	PLAT	Plasminogen activator, tissue	HGNC:9051
22	PDGFRA	Platelet-derived growth factor receptor, alpha polypeptide	HGNC:8803
23	TNF-a	Tumor necrosis factor	HGNC:11892
Transcription factors			
24	AHR	Aryl hydrocarbon receptor	HGNC:348
25	FOXP3	Forkhead box P3	HGNC:6106
26	GATA-3	GATA binding protein 3	HGNC:4172
27	STAT3	Signal transducer and activator of transcription 3	HGNC:11364
28	SOCS3	Suppressor of cytokine signaling 3	HGNC:19391
29	RELB	V-rel avian Reticuloendotheliosis viral oncogene homlog B	HGNC:9956
30	RELA	V-rel avian reticuloendotheliosis viral oncogene homolog A	HGNC:9955
Purinergic receptors			
31	ADORA1	Adenosine A1 receptor	HGNC:262
32	Adora2a	Adenosine A2a receptor	MGI:99402
33	Adora2b	Adenosine A2b receptor	MGI:99403
34	ADORA3	Adenosine A3 receptor	HGNC:268
35	P2RX1	Purinergic receptor P2X, ligand-gated ion channel, 1	HGNC:8533
36	P2RX2	Purinergic receptor P2X, ligand-gated ion channel, 2	HGNC:15459
37	P2RX3	Purinergic receptor P2X, ligand-gated ion channel, 3	HGNC:8534
38	P2RX4	Purinergic receptor P2X, ligand-gated ion channel, 4	HGNC:8535
39	P2RX5	Purinergic receptor P2X, ligand-gated ion channel, 5	HGNC:8536
40	P2RX7	Purinergic receptor P2X, ligand-gated ion channel, 7	HGNC:8537
41	P2RY1	Purinergic receptor P2Y, G-protein coupled, 1	HGNC:8539
42	P2RY11	Purinergic receptor P2Y, G-protein coupled, 11	HGNC:8540

TABLE 1 (*Continued*)

No.	Symbol	Official Full Name	Source http://www.genenames.org/data/hgnc_data.php?hgnc_id=262
43	P2RY12	Purinergic receptor P2Y, G-protein coupled, 12	HGNC:18124
44	P2RY13	Purinergic receptor P2Y, G-protein coupled, 13	HGNC:4537
45	P2RY14	Purinergic receptor P2Y, G-protein coupled, 14	HGNC:16442
46	P2RY2	Purinergic receptor P2Y, G-protein coupled, 2	HGNC:8541
47	P2RY4	Pyrimidinergic receptor P2Y, G-protein coupled, 4	HGNC:8542
48	P2RY6	Pyrimidinergic receptor P2Y, G-protein coupled, 6	HGNC:8543
Purinergic enzymes			
49	NT5E	5′-nucleotidase, ecto (CD73)	HGNC:8021
50	ADA1	Adenosine deaminase	HGNC:186
51	AMPD2	Adenosine monophosphate deaminase 2	HGNC:469
52	AMPD3	Adenosine monophosphate deaminase 3	HGNC:470
53	CECR1	Cat eye syndrome chromosome region, candidate 1	HGNC:1839
54	DDP4	Dipeptidyl-peptidase 4	HGNC:3009
55	ENTPD1	Ectonucleoside triphosphate diphosphohydrolase 1	HGNC:3363
56	ENTPD2	Ectonucleoside triphosphate diphosphohydrolase 2	HGNC:3364
57	ENTPD3	Ectonucleoside triphosphate diphosphohydrolase 3	HGNC:3365
58	NADSYN1	NAD synthetase 1	HGNC:29832
59	NMNAT1	Nicotinamide nucleotide adenylyltransferase 1	HGNC:17877
60	NMRK1	Nicotinamide riboside kinase 1	HGNC:26057
Vesicular transport proteins			
61	SYP	Synaptophysin	HGNC:11506
62	SNAP25	Synaptosomal-associated protein, 25 kDa	HGNC:11132
63	SYT1	Synaptotagmin I	HGNC:11509
64	SYT2	Synaptotagmin II	HGNC:11510
65	STX1A	Syntaxin 1A (brain)	HGNC:11433
66	USO1	USO1 vesicle docking protein homolog	HGNC:30904
Cation channels			
67	CACNA1B	Ca^{2+} channel, voltage-dependent, N type, alpha 1B	HGNC:1389
68	KCNE1	K^{+} voltage-gated channel, Isk- member 1	HGNC:6240
69	PANX1	Pannexin 1	HGNC:8599
70	TRPV1	Transient receptor potential cation channel, V1	HGNC:12716
71	TRPA1	Transient receptor potential cation channel, A, member 1	HGNC:497
72	CHRNA7	α7 nicotinic receptor	HGNC:1960
Enzymes and signaling pathways			
73	PRKACA	cAMP-dependent PKA	HGNC:9380
74	CASP3	Caspase 3, apoptosis-related cysteine peptidase	HGNC:1504
75	HMOX1	Heme oxygenase (decycling) 1	HGNC:5013
76	NOS2	Nitric oxide synthase 2, inducible	HGNC:7873
77	PDE4B	Phosphodiesterase 4B, cAMP-specific	HGNC:8781
78	PRKCε	Protein kinase C, epsilon	HGNC:9401
79	SOD2	Superoxide dismutase 2, mitochondrial	HGNC:11180
80	TPH1	Tryptophan hydroxylase 1	HGNC:12008
81	TPH2	Tryptophan hydroxylase 2	HGNC:20692
Receptors and proteins			
82	ADIPOR1	Adiponectin receptor 1	HGNC:24040
83	ADIPOR2	Adiponectin receptor 2	HGNC:24041

TABLE 1 (*Continued*)

No.	Symbol	Official Full Name	Source http://www.genenames.org/ data/hgnc_data.php?hgnc_id=262
84	APOE	Apolipoprotein E	HGNC:613
85	AGTR1A	Angiotensin II receptor, type 1	HGNC:336
86	AGTR2	Angiotensin II receptor, type 2	HGNC:338
87	CDH1	Cadherin 1, type 1, E-cadherin (epithelial)	HGNC:1748
88	CTNNB1	Catenin (cadherin-associated protein), β 1	HGNC:2514
89	CLDN1	Claudin 1	HGNC:2032
90	CLDN3	Claudin 3	HGNC:2045
91	CLDN5	Claudin 5	HGNC:2047
92	GMCSF	Colony stimulating factor 2 (granulocyte-macrophage)	HGNC:2434
93	GFAP	Glial fibrillary acidic protein	HGNC:4235
94	GUSB	Glucuronidase, beta	HGNC:4696
95	HP	Haptoglobin	HGNC:5141
96	HGF	Hepatocyte growth factor	HGNC:4893
97	IGFBP5	Insulin-like growth factor binding protein 5	HGNC:5474
98	OCLN	Occludin	HGNC:8104
99	PIGR	Polymeric immunoglobulin receptor	HGNC:8968
100	PSMC3	Proteasome 265 subunit, ATPase3	HGNC:9549
101	RBP1	Retinol binding protein 1, cellular	HGNC:9919
102	S100B	S100 calcium binding protein B	HGNC:10500
103	TACR1	Tachykinin receptor 1	HGNC:11526
104	TBX21	Thromboxin 21	HGNC:11599
105	TGFB1	Transforming growth factor, beta 1	HGNC:11766
106	VSNL1	Visinin-like 1	HGNC:12722
107	VDR	Vitamin D3 receptor	HGNC:12679

direct detection of target molecules using color-coded molecular barcodes, providing a digital simultaneous quantification of the number of target molecules. Total (RNA 100 ng) was hybridized overnight with nCounter Reporter (20 μL) probes in hybridization buffer and in excess of nCounter Capture probes (5 μL) at 65°C for 16−20 hours. The hybridization mixture containing target/probe complexes was allowed to bind to magnetic beads containing complementary sequences on the capture probe. After each target found a probe pair, excess probes were washed, followed by a sequential binding to sequences on the reporter probe. Biotinylated capture probe–bound samples were immobilized and recovered on a streptavidin-coated cartridge. The abundance of specific target molecules was then quantified using the nCounter digital analyzer. Individual fluorescent barcodes and target molecules present in each sample were recorded with a CCD camera by performing a high-density scan (600 fields of view). Images were processed internally into a digital format and were normalized using the NanoString nSolver Software analysis tool. Counts were normalized for all target RNAs in all samples based on the positive control RNA, to account for differences in hybridization efficiency and posthybridization processing including purification and immobilization of complexes. The average was normalized by background counts for each sample obtained from the average of the 8 negative control counts. Subsequently, a normalization of mRNA content was performed based on internal reference housekeeping genes Gusb, TBP, NMNAT1, RBP1, STX1A, and CTNNB1 using nSolver Software (NanoString Technologies).

LPS Induction and Detection of ATP Secretion Using the Luciferin–luciferase Assay

Luciferin–luciferase assay was used to monitor basal secretion of ATP according to the manufacturer's instructions (ATP-lite, Perkin Elmer, Waltham, MA) using 100 μL of the supernatant.

EGCs were grown in 12-well dishes (2×10^4 cells in each well) in DMEM supplemented with 10% FBS and 1% penicillin–streptomycin, until confluence was reached (7–10 d). Cell cultures were grown individually from 4 different surgical specimens and were used at passages 4 to 7. EGCs isolation was performed from MP of 3 surgical patients (2 jejunum, 1 colon) and SMP of 1 patient (colon). Preliminary analysis did not reveal any differences in amount of ATP secretion in each surgical specimen and therefore, data in different surgical specimens were pooled

together. To study the effect of treatment on ATP secretion, cells were incubated with LPS+IFN-γ in 400 μL of DMEM with 10% FBS and 1% penicillin–streptomycin. For controls, the medium alone was used. Supernatants (300 μL) were collected and immediately frozen in liquid nitrogen for measurement of ATP (ATP-lite, Perkin Elmer).

LPS Induction and Detection of s100β Protein Secretion

The secretion of s100β was detected in a100 μL supernatant sample using an enzyme-linked immunosorbent assay kit (#RD192090100R, Biovendor LLC, Asheville, NC) according to the manufacturer's instructions. The secretion of s100β protein was done in the same supernatant samples as those used for ATP release (see above protocol).

Experimental Strategies (additional information is included in Figs. 1–8)

1. LPS (LPS+IFN-γ) induction was used as a way to induce inflammation in hEGC and evaluate (1) molecular signaling by nanostring analysis, (2) mechanosensitivity by monitoring Ca^{2+} signals with fluo-4/Ca^{2+} imaging, (3) Ca^{2+} handling, (4) ATP Ca^{2+} responses, and (5) secretion of mediators from hEGC.
2. LPS induction (LPS+IFN-γ) was used to evaluate the rhEGC phenotype, and identify the mRNA signature profile in response to inflammation for a custom panel of 107 genes listed in Table 1.
3. LPS induction (LPS+IFN-γ) was used to evaluate the impact of inflammation on secretion of the purinergic gliotransmitter ATP and the glial protein s100β.
4. LPS induction (LPS+IFN-γ) was used to evaluate the impact of inflammation on mechanical-evoked Ca^{2+} responses in response to increase in perfusion flow from 2 mL/min to 10 mL/min. We found in preliminary experiments that increase in flow induces Ca^{2+} oscillations in hEGC in culture.[11] Therefore, we tested the effect of LPS induction on flow-dependent Ca^{2+} oscillations. Cells responded in 3 different ways to increase in flow: (1) in cells with no oscillations (quiescent/flat line) at 2 mL/min (low flow), increase in flow to 10 mL/min could elicit oscillations, (2) in cells with Ca^{2+} oscillations at 2 mL/min (low flow), an increase in flow to 10 mL/min did not cause any further response, and (3) in cells with low flow oscillations, increase in flow caused a change in the pattern of oscillations.
5. LPS induction was used to evaluate the effect of inflammation on exogenous ATP-induced Ca^{2+} responses to 100 μM ATP perfusion for 1 to 2 minutes. Peak Ca^{2+} responses and occurrence of Ca^{2+} transients were analyzed in response to LPS.
6. LPS induction was used to evaluate the effect of inflammation on store-operated Ca^{2+} entry (SOCE) into hEGC. The protocol used involved inducing Ca^{2+} oscillations by increasing the flow rate, and then blocking Ca^{2+} oscillations by perfusing 0.0Ca^{2+} buffer (+200 μM ethylene glycol-bis (β-aminoethyl ether)-N,N,$N^{1,N}{}_1$-tetraacetic acid (EGTA)) to block Ca^{2+} entry. Re-introduction of Ca^{2+} to the Krebs buffer (2 mM $CaCl_2$) elicits a robust Ca^{2+} response by stimulating Ca^{2+} entry through SOCE channels that are activated by Ca^{2+} depletion. The magnitude or occurrence of the SOCE response was measured and compared between LPS treatment and control. Note: ATP Ca^{2+} responses occur in the absence of extracellular Ca^{2+}, and influence of LPS on ATP responses was tested in this protocol as well (in some experiments).

Cell Viability Assay

Cell viability was tested in cell cultures using the NuclearID Blue-green cell viability reagent (ENZO, Farmingdale, NY) following the protocol for adherent cells.

Immunocytochemistry

To confirm the identity of glial cells in our hEGC cultures, immunofluorescent labeling was done for glial markers (s100β, glial fibrillary acidic protein GFAP), smooth muscle/epithelial actin, or fibroblasts. hEGCs were fixed in 4% paraformaldehyde for 15 minutes at room temperature, rinsed 3 times with cold phosphate-buffered saline (PBS) 0.1 M and placed at 4°C until further processing. Cells were treated with 0.5% Triton X, 10% normal donkey serum in PBS to permeabilize the cells and block nonspecific antibody binding for 30 minutes at room temperature. Primary antibodies were diluted in PBS-0.1% Triton X, and 2% normal donkey serum, and were incubated with cells overnight (18–24 h) at 4°C. Next day preparations were rinsed 3 times in 0.1M PBS/1 minute and incubated 60 minutes at room temperature in secondary antibodies diluted in PBS-0.1%, Triton X, and 2% normal donkey serum. Monoclonal mouse anti-S100β antibody (1:100–1:500 dil., cat #ab11178; Abcam, Cambridge, MA), mouse monoclonal anti-α smooth muscle/epithelial actin antibody (1:50–1:500 dil., cat #ab18147; Abcam), rabbit anti-GFAP antibody (1:500 dil., cat #z0334; DAKO, Carpinteria, CA), and monoclonal mouse antifibroblast/epithelial cell antibody (1:100–1:500 dil., cat #NB600–777; Novus Biologicals, Littleton, CO) were used for analysis. Alexa Fluor 488 or 568 donkey anti-mouse or anti-rabbit secondary antibodies were used at a dilution of 1:400 (Cambridge, MA). Omission of primary antibodies was used to test for background staining of the secondary antibodies. Preabsorption of primary antisera with immunogenic peptides abolished immunoreactivity. Data confirmed previous reports by Turco et al,[7] and is not shown, except for illustrating that cells express s100β immunoreactivity.

Statistics

Nanostring data was normalized in nSolver 2.5 according to manufacturer recommendations. Two-tailed Student's *t* tests were used to test for significant difference in gene expression between control and LPS. Box plots were created to depict differential gene expression between control and LPS tissue on their original scale. Data is reported as a fold change in gene expression,

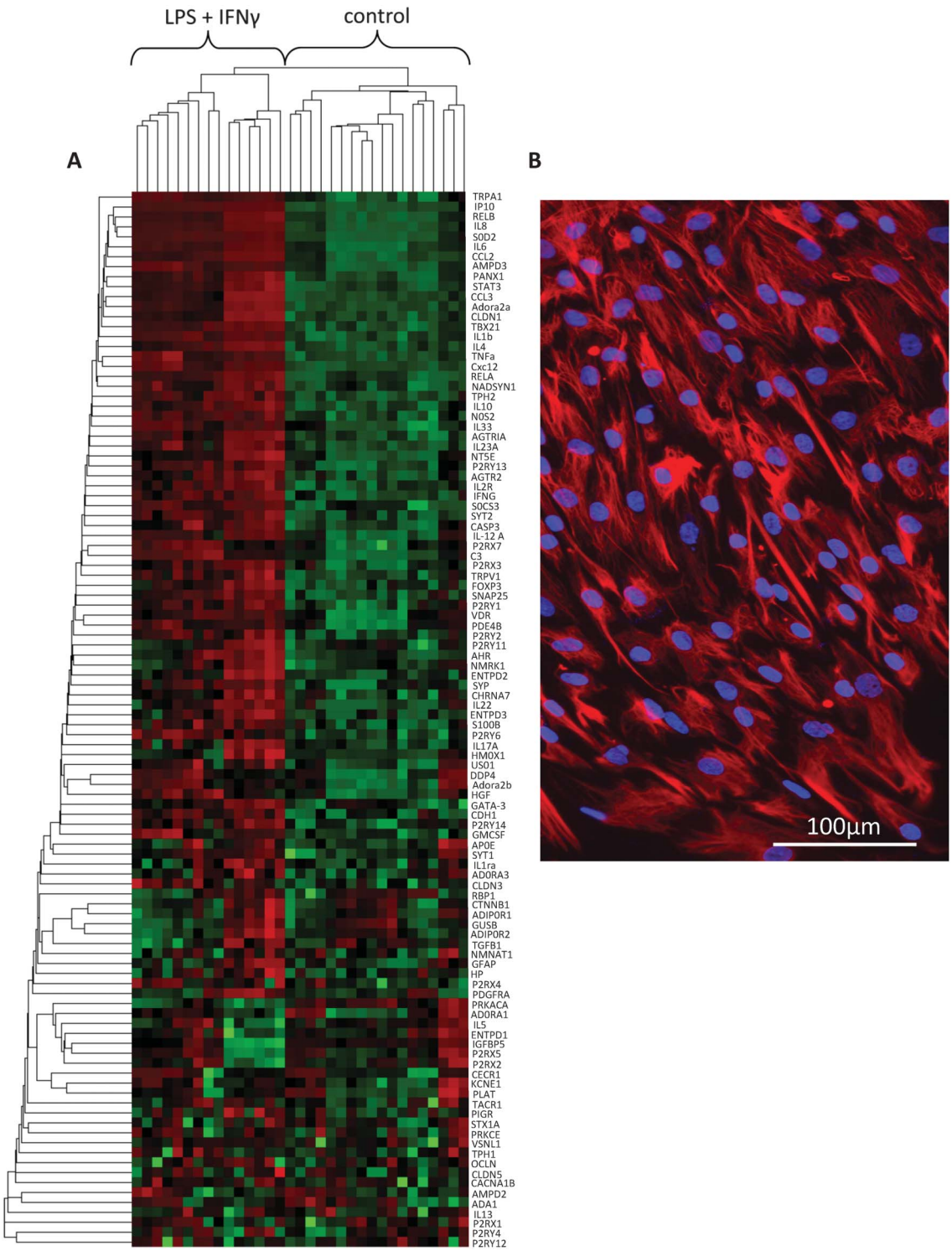

FIGURE 1. Gene expression changes in hEGC induced by bacterial LPS+IFN-γ stimulation. A, Heat map of the normalized mRNA counts of unstimulated (control) and stimulated (LPS+IFN-γ) hEGC of each sample. The colors of the heat map refer to expression level with respect to the mean for a gene across all the samples (green is lower than the mean and red is above). Data is Z-score transformed for each gene. Dendrograms (clusters) are shown for sample clustering (top of figure) and for gene clustering (left side of figure). Human EGC were plated at 20,000 cells/dish and grown to a confluent culture. Cells were incubated with LPS+IFN-γ for 24 hours. Gene expression levels in hEGC were determined for a custom panel of 107 genes using Nanostring probe-based analysis of 100 ng of total RNA in multiple samples from each of 4 patients. B, s100B immunoreactivity in hEGC (4′,6′-diamidino-2-phenylindole [DAPI] nuclear counter-stain, blue).

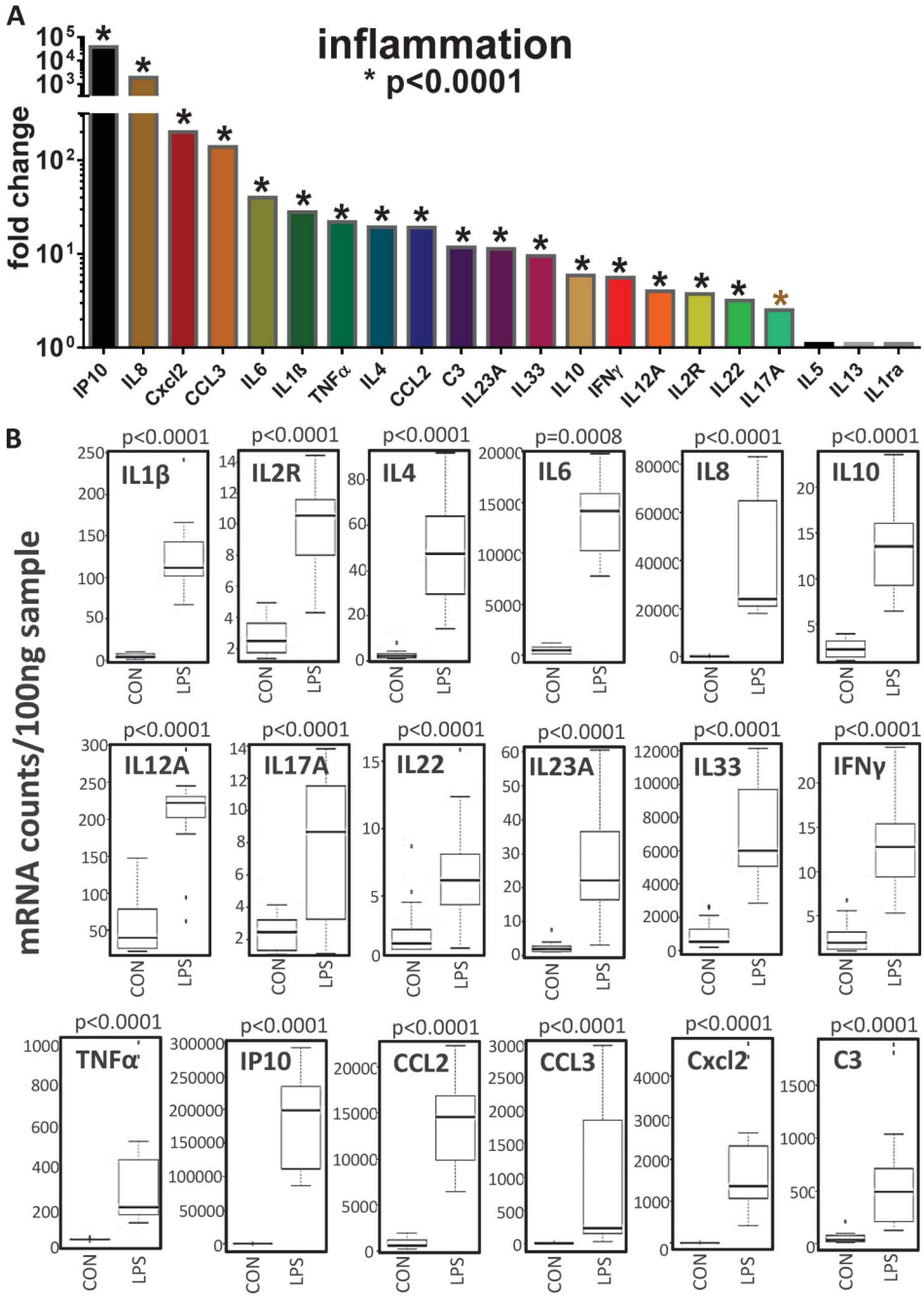

FIGURE 2. Gene expression changes in inflammatory genes induced by bacterial LPS+IFN-γ stimulation in hEGC. A, Fold change in normalized gene expression for chemokine and cytokine genes. Discoveries (*) were determined by false discovery rate following multiple *t* test analysis; *significant fold increase in mRNA expression in response to treatment, at $P < 0.0001$. B, Box plots of mRNA counts/100 ng sample showing differences in gene expression between control (CON, unstimulated) and LPS (stimulated) samples of hEGC (n = 12–16 samples of hEGC obtained from GI surgical specimens of 4 human subjects).

mRNA counts/100 ng total RNA sample, or $\log_2$ mRNA counts for each of 107 genes analyzed by nanostring. Differences between control and treatment groups are significant at $P < 0.01$ to take into consideration that ~100 different genes were being analyzed (Most changes observed in our study were significant at a $P < 0.0001$).

Chi-square analysis was used to analyze data for effects of treatment (LPS+IFN-γ) on Ca^{2+} oscillations, MS, ATP responses, and SOCE responses (i.e., restore normal 2 mM Ca^{2+} in the Krebs buffer solution). A 2-tailed Student's *t* test was used to evaluate differences between control and treatment for ATP release and s100β protein release from hEGC.

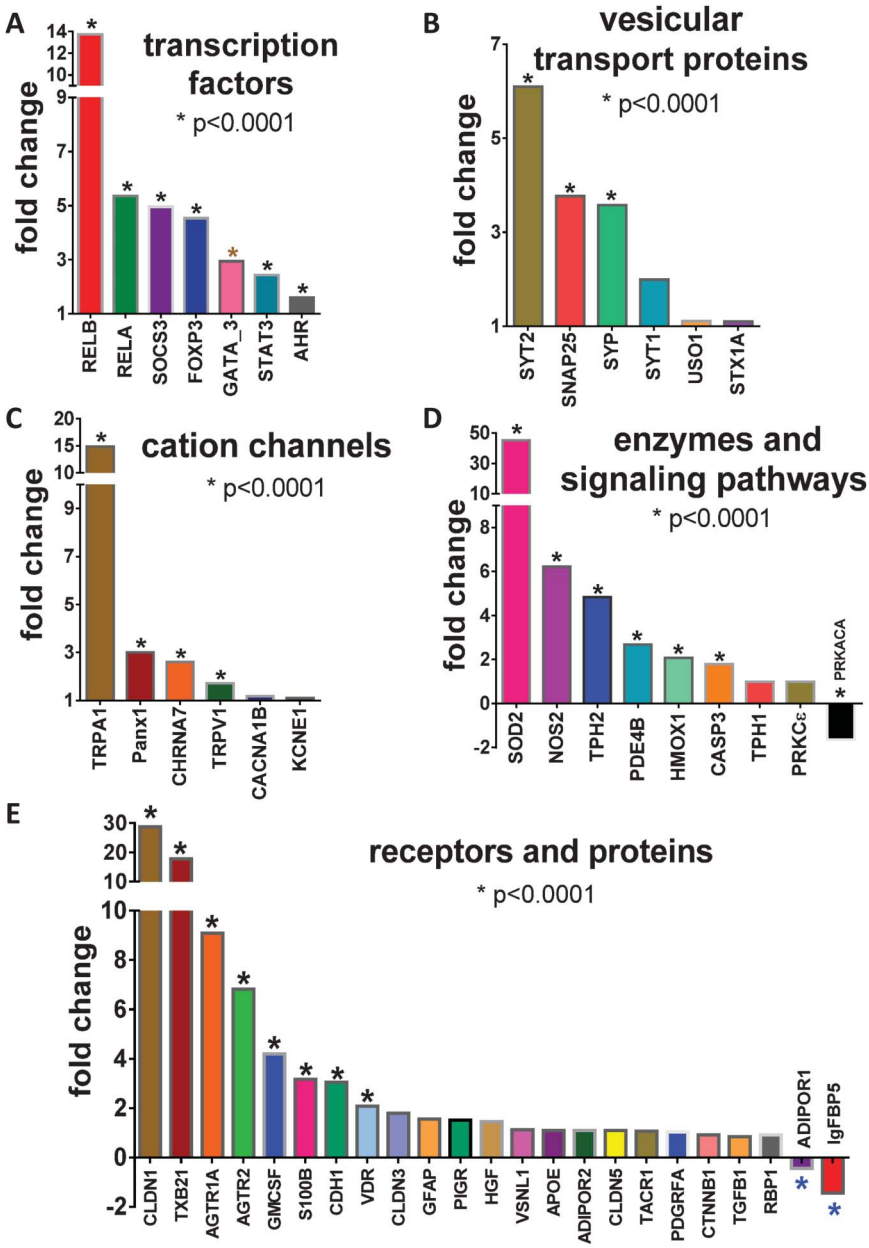

FIGURE 3. Gene expression changes induced by bacterial LPS+IFN-γ stimulation in hEGC for (A) transcription factors, (B) vesicular transport proteins, (C) cation channels, (D) enzymes and signaling pathways, (E) receptors and proteins. Data represent fold changes in normalized gene expression. Discoveries (*) were determined by false discovery rate following multiple *t* test analysis; *significant fold increase in mRNA expression in response to treatment, at $P < 0.0001$ (n = 12–16 samples of hEGC obtained from GI surgical specimens of 4 human subjects). The box-plots of mRNA counts/100 ng sample showing differences in gene expression in response to treatment are included in Figs. 1 and 2, Supplemental Digital Content 1, http://links.lww.com/IBD/B301.

Heat Map Analysis

A heat map was generated in nSolver from normalized data of individual samples in control or treatment group (LPS+IFN-γ). The colors of the heat map refer to expression level with respect to the mean for a gene across all the samples (green is lower than the mean and red is above). By default, the data is Z score transformed for each gene so that all of the means and standard deviations of all of the genes line up. Thus a 2-fold increase in expression will look the same for a gene expressed at hundreds of counts versus one expressed in the hundreds of thousands. Dendrograms (clusters) were created for genes and samples in nSolver using agglomerative clustering. Eucledian distance was used to look for similarities between clusters. Centroid methodology was used to link clusters together. The linkage method (how values are

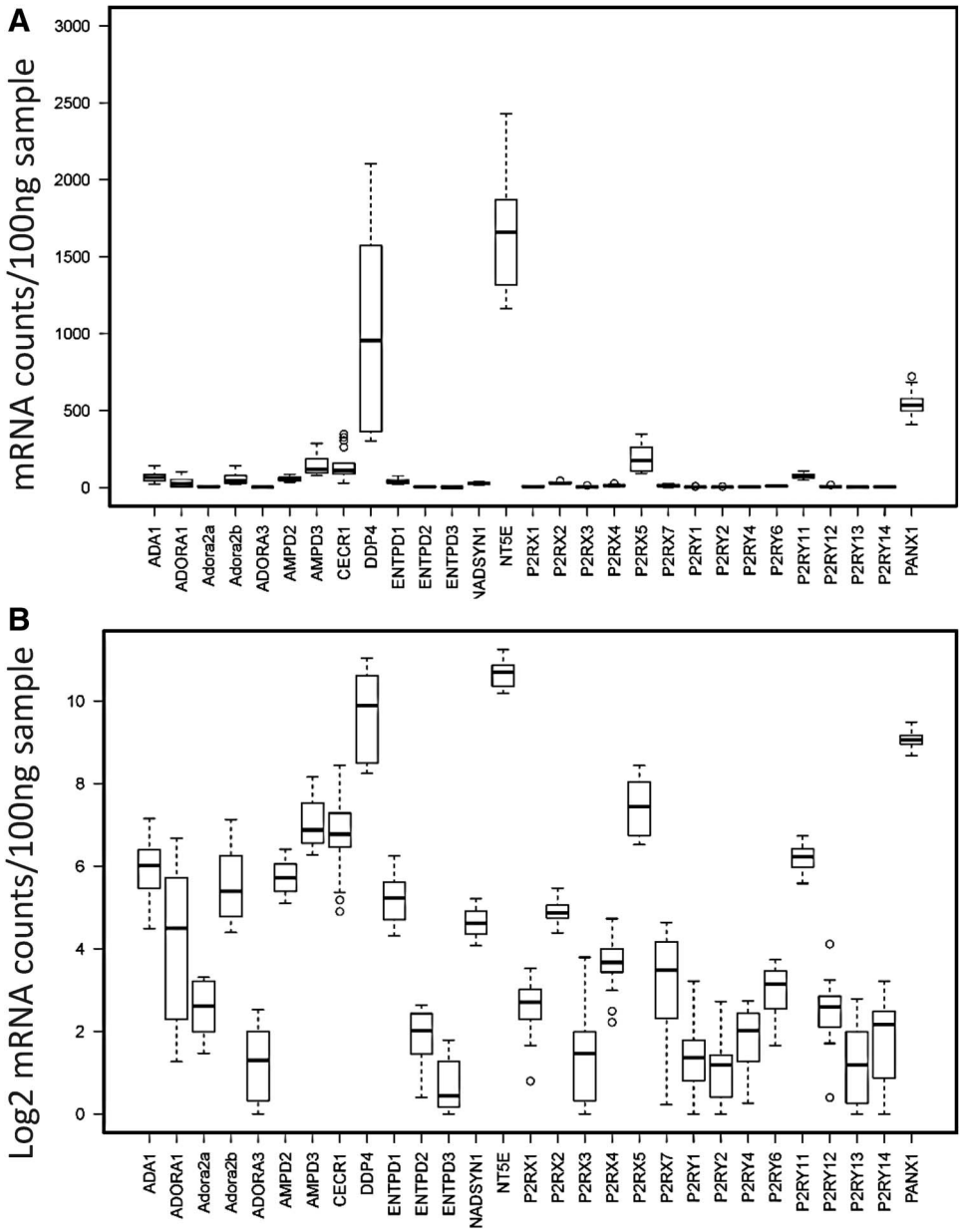

FIGURE 4. The gene expression profile of 29 purine genes involved in purinergic signaling pathways, including adenosine receptors, P2X-receptors, P2Y receptors, and enzymes involved in metabolic degradation of purine nucleotides, and di-nucleotides. A, Box-plots of gene expression for mRNA counts/100 ng sample. DDP4 and NT5E have the highest expression in hEGC. B, Box-plots of gene expression displayed on a $\log_2$ scale for mRNA counts better revealed differences in mRNA expression of control (unstimulated) hEGC.

assigned to a branch containing multiple genes) used centroid methodology.

Interactions Between Purines and Inflammatory Genes

General linear models were fit with main effects for purine group and inflammatory markers, and we tested whether there was an interaction between the 2 variables, by evaluating whether the effect of each inflammatory gene on purine gene was significantly different by study group. Separate models were fit for each outcome (purine gene) and predictor (inflammatory gene) combination. Significance was adjusted by controlling the mean number of false positives. Significance was accepted at $P = 0.01$ to correct for multiple comparisons. Statistical software SAS 9.3 and R was used for analysis.

RESULTS

Data is summarized in Figures 1–9, Figs. 1 and 2, Supplemental Digital Content 1, http://links.lww.com/IBD/B301,

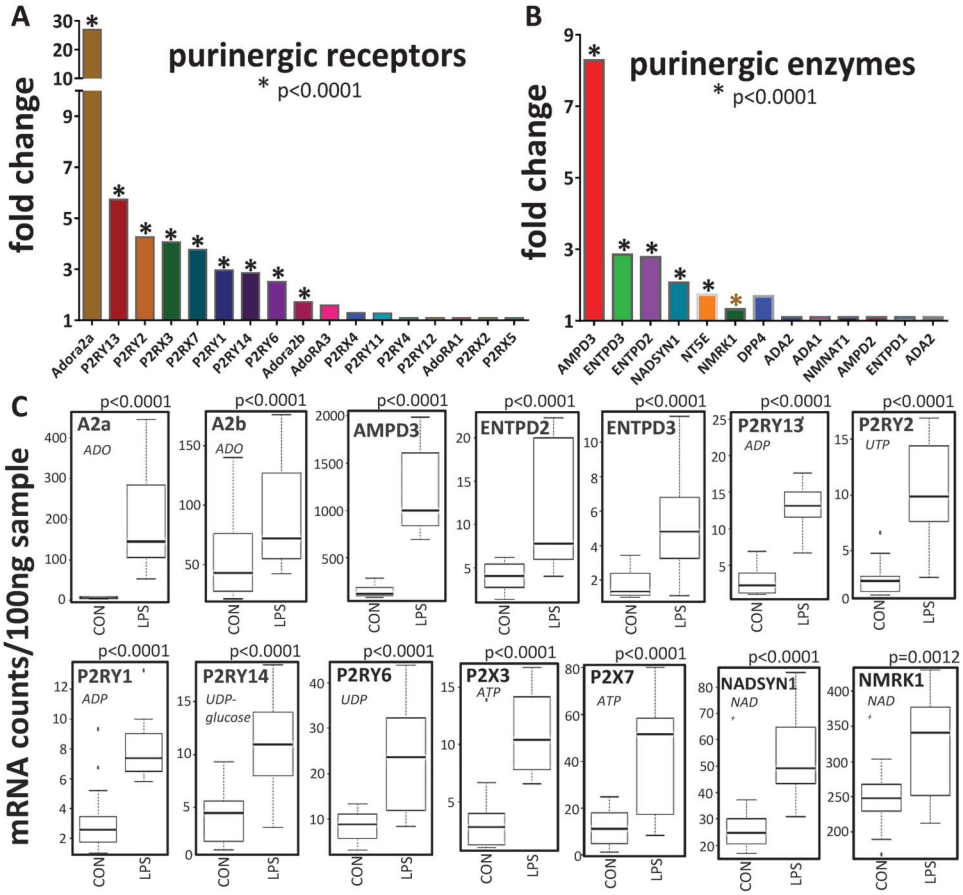

FIGURE 5. Gene expression changes in purine genes induced by bacterial LPS+IFN-γ stimulation in hEGC. A, Fold changes in normalized gene expression for purinergic receptor genes. B, Fold changes in gene expression for purinergic enzymes involved in metabolic degradation of purines. Discoveries (*) were determined by false discovery rate following multiple *t* test analysis; *significant fold increase in mRNA expression in response to treatment, at $P < 0.0001$. C, Box plots of mRNA counts/100 ng sample showing differences in gene expression between control (CON, unstimulated) and LPS (stimulated) samples of hEGC (n = 12–16 samples of hEGC obtained from GI surgical specimens of 4 human subjects).

Tables 1 and 2, and Tables 1–3, Supplemental Digital Content 2, http://links.lww.com/IBD/B302. Nanostring analysis was used to evaluate the impact of inflammation (LPS+IFN-γ) on gene expression in hEGC. The code set included a custom-designed set of 107 genes associated with IBDs (Table 1) representing mRNA gene expression for inflammatory genes, purinergic signaling genes, vesicular release proteins, neurotransmitters, sensory signaling genes, transcription factors, postreceptor signaling enzymes, and genes linked to free radical pathways. A heat map showing the molecular signature of the "rhEGC phenotype" is shown in Figure 1A. Cells are immunoreactive for the glial Ca^{2+} binding protein s100β (Fig. 1B).

LPS induced a "rhEGC phenotype" and caused upregulation in mRNA transcripts of 58% of 107 genes including subsets of inflammatory genes (54%), purine genes (52%), channels (40%), vesicular transport, transcription factors, free radical/other pathway genes; 95% of these mRNAs were upregulated by LPS treatment; only 3 mRNAs were downregulated by treatment.

LPS Induction of Inflammatory Pathways

LPS induction caused mRNA up-regulation in inflammatory genes. These included 7 chemokines (IP10, IFN-γ, CxCl2, CCl3, CCl2, C3, and s100B), 12 cytokines (IL-1β, IL-2R, tumor necrosis factor [TNF]-α, IL-4, IL-6, IL-8, IL-10, IL-12A, IL-17A, IL-22, IL-23A, and IL-33), and 2 growth factors (IGFBP5 and GMCSF). Fold changes (~ranging from 3-fold to 1900-fold increase in mRNA expression) for inflammatory genes are summarized in Figure 2 and Table 1, Supplemental Digital Content 2, http://links.lww.com/IBD/B302.

LPS Induction of Transcription Factors

Several transcription factors were up-regulated by LPS induction (Fig. 3A). RELB and RELA, transcription factors involved in NFkB induction were up-regulated by 14-fold and 5-fold, respectively. Other transcription factors including suppressor of cytokine signaling 3 (SOCS3), forkhead box P3 (FOXP3), GATA_3, signal transducer and activator of transcription 3 (STAT3), and aryl hydrocarbon receptor were also up-regulated several fold (2–5-fold).

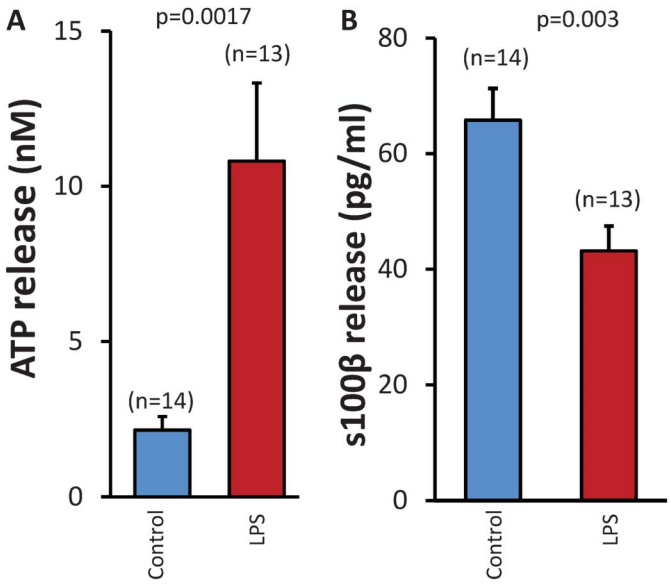

FIGURE 6. Basal release of mediators was altered in hEGC treated for 24 hours with bacterial LPS and IFN-γ. A, Treatment increased basal release (unstimulated) of the purinergic gliotransmitter ATP from hEGC ($P = 0.0017$). B, In contrast, the same treatment with LPS and IFN-γ caused a significant reduction in s100β release ($P = 0.003$). Data is presented as mean ± SEM for 13 to 14 samples for each condition. Data represents pooled culture results from hEGC obtained from surgical specimens of 4 human subjects.

Vesicular Transport Proteins

Gene mRNA expression of vesicular transport proteins were up-regulated by LPS induction. SYT2 was upregulated by 6-fold, followed by SNAP25 (+4-fold) and SYP (+4-fold). SYT1, US01, and STX1A were not affected by treatment (Fig. 3B).

Cationic Channels

There was a 15-fold up-regulation of the sensory TRPA1 channel (transient receptor potential A1) in hEGC. In contrast, the TRPV1 channel (transient receptor potential V1) was only marginally up-regulated by treatment (+1.72-fold). The hemi-channel pannexin 1 (Panx1) and the α7-nicotinic cholinergic channel (CHRNA7) were up-regulated ~ 3-fold by treatment. Expression of other channels (CACNA1B/N-type Ca^{2+} channel, KCNE1/K^+ channel or TACR1/tachykinin receptor/not shown) remained the same (Fig. 3C).

Enzymes, Signaling, and Free Radical Pathways

Free radical pathway enzymes were highly up-regulated in hEGC in response to LPS induction. These included SOD2 (increase 45-fold), NOS2 (+6-fold), TXB21 (+18-fold), and heme oxygenase-1 (HMOX1) (+2-fold). Caspase 3, an enzyme involved in apoptosis was up-regulated marginally by 1.78-fold.

The expression of a number of other signaling pathway enzymes and proteins were affected by LPS induction. The calcium binding protein s100β was up-regulated by 3-fold, but the expression of GFAP remained the same. PRKCε was not altered. CDH1 (E-cadherin) was up-regulated by 3-fold. The cAMP-dependent protein kinase-A enzyme PRKACA was the only enzyme that was down-regulated by LPS induction ($P < 0.0001$). The cyclic adenosine 3′,5′-monophosphate (cAMP)-dependent phosphodiesterase (PDE) 4B enzyme was up-regulated by 3-fold in response to LPS. The expression of mRNA for enzymes involved in the metabolism of serotonin was selectively up-regulated by LPS induction. The mRNA transcripts for tryptophan hydroxylase (TPH) 2 enzyme for the metabolism of serotonin was up-regulated by 5-fold, whereas the expression of the TPH1 enzyme, known to be highly expressed in enterochromaffin cells remained the same (see Supplemental Table 3, Supplemental Digital Content 2, http://links.lww.com/IBD/B302).

Expression of Other Receptors and Proteins

Expression of angiotensin receptors AT1A (AGTRIA) and AT2A (AGTR2) were up-regulated 9-fold and 7-fold, respectively. The vitamin D_3 receptor was up-regulated 2-fold. The mRNA expression for several barrier (tight-junction) proteins was increased by LPS induction. Claudin (CLDN)1 mRNA expression was increased by 29-fold and CDH1 by 3-fold; mRNA expression of CLDN3, CLDN5, and VSNL1 was not significantly altered by LPS (see Supplemental Table 3, Supplemental Digital Content 2, http://links.lww.com/IBD/B302).

Expression and Detection of mRNA Transcripts for Purinergic Genes in hEGC

Differential and relative expression of mRNAs for various purine genes in hEGCs suggests that a complex array of potential purinergic signaling mechanisms operate in hEGCs (Fig. 4A, B). The mRNA expression profile for purinergic signaling genes was revealed by nanostring analysis of 29 purine genes including P1, P2X, P2Y receptors and enzymes involved in metabolic pathways for endogenous purines (ATP, uridine triphosphate [UTP], adenosine diphosphate [ADP], adenosine [ADO], β-nicotinamide adenine dinucleotide [NAD]). The mRNA counts for 100 ng of total RNA/sample indicate that NT5E (CD73) has the highest expression of all purine genes, followed by dipeptidyl-peptidase 4 (DDP4), adenosine monophosphate deaminase (AMPD) 3, P2XR5, and adenosine deaminase (ADA) 2. All 29 purine genes were expressed in hEGCs (Fig. 4A, B).

LPS Induction of Purinergic Signaling Pathways

Data for purine genes with significant up-regulation in response to LPS induction are summarized in Figure 5A for purinergic receptors and Figure 5B for purinergic enzymes. Table 2, Supplemental Digital Content 2, http://links.lww.com/IBD/B302 includes the fold-changes in mRNA expression for purine genes.

LPS induction did not have any effect on the mRNA expression in 12 of 29 purine genes (41.3%) including ADOA3, ENTPD1, P2RX2, DDP4, P2RX4, P2RY12, ADORA1, ADA1, P2RX1, P2RY4, CECR1 (ADA2). LPS induction causes

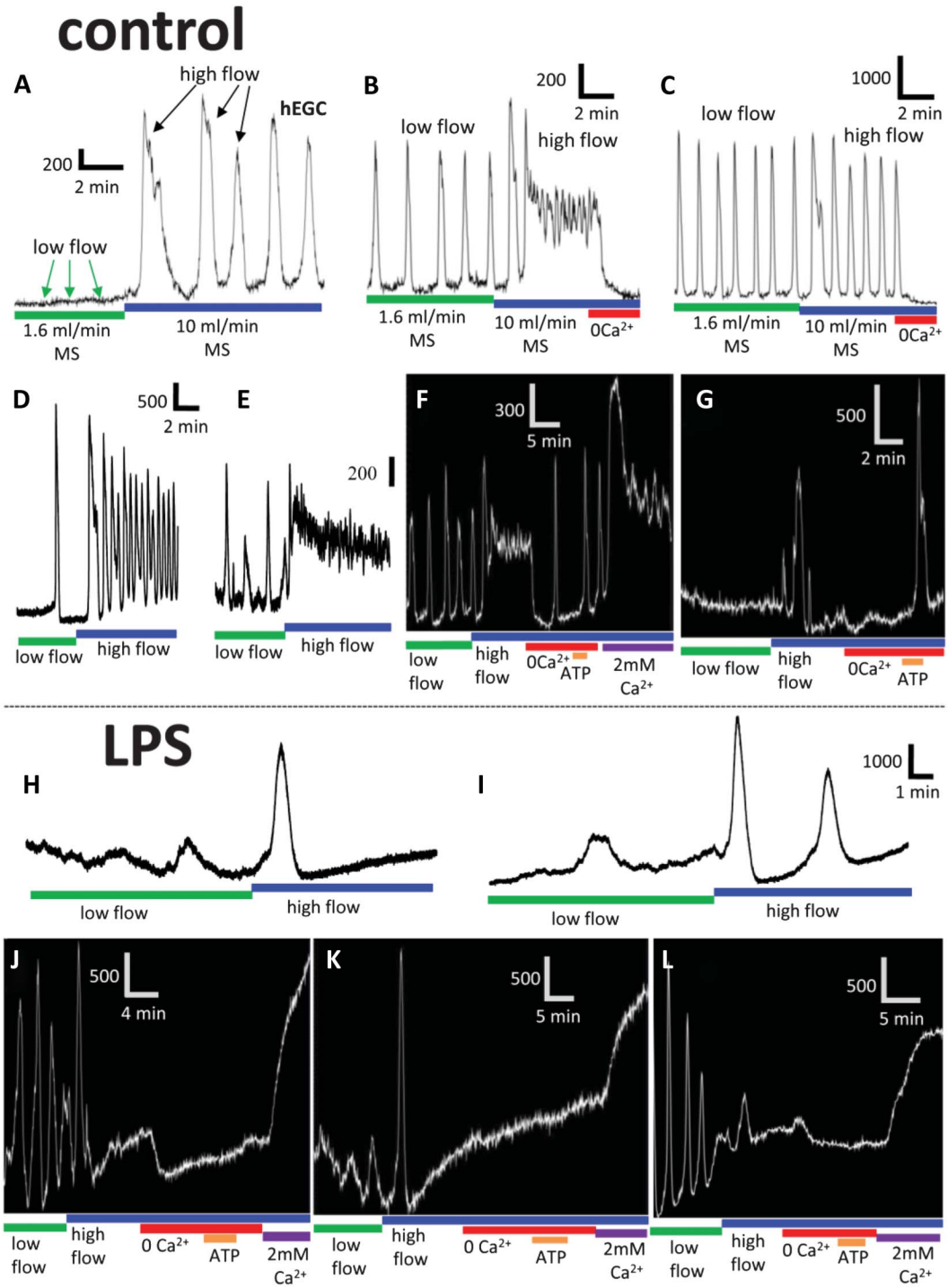

FIGURE 7. Ca^{2+} responses and flow-dependent Ca^{2+} responses in hEGC are disrupted by bacterial LPS treatment. (A–G) Control cell Ca^{2+} responses. A, A typical example of a control hEGC that responds to increasing pulsatile flow of the peristaltic pump from 1.6 mL/min to 10 mL/min. Flow induces rhythmic Ca^{2+} oscillations. Change in flow is used as a physiologic mechanical stimulus (MS) to trigger Ca^{2+} oscillations. The cell does not have oscillations at low flow. B, Another cell depicting oscillations at low flow. Increasing flow changes the pattern of the oscillations, and the response is entirely dependent on extracellular Ca^{2+} levels since 0.0 Ca^{2+} + ethylene glycol-bis(β-aminoethyl ether)-N,N,$N^{1,N}{}_1$-tetraacetic acid (EGTA) buffer abolishes the response. C, Example of a cell that displays rhythmic Ca^{2+} oscillations at low flow and does not change its response with increase in flow. The oscillations depend on extracellular Ca^{2+}levels. D, Example of a cell with a single Ca^{2+} transient at low flow and a high frequency Ca^{2+} oscillation at high flow. E, A cell displaying distinct Ca^{2+} responses at low and high flow. F, Example of another cell responding to change in flow. Rarely, Ca^{2+} spikes can occur in 0.0 Ca^{2+} + EGTA (≤10% of hEGC). The ATP-induced Ca^{2+} response does not depend on

significant mRNA up-regulation in 17 of 29 purine genes (59.7%). Up-regulation occurred in Adora2a (27-fold), AMPD3 (8-fold), P2RY13 (6-fold), P2RY2 (4-fold), P2RX3 (4-fold), P2RX7 (3.8-fold), P2RY1 (3-fold), Panx1 (3-fold), P2RY14 (2.9-fold), ENTPD3 (2.9-fold), ENTPD2 (2.8-fold), P2RY6 (2.5-fold), NADSYN1 (2.1-fold), NT5E (1.7-fold), NMRK1 (1.3-fold), P2Y11 (1.3-fold), and Adora2b (1.7-fold). None of the purine genes showed any down-regulation.

Significant Interactions Between Purine Genes and Inflammatory Genes

Analysis of the change in slope of the linear relationship between mRNA expression in purine genes versus inflammatory genes between control and LPS-treated hEGC was used to determine significant interactions. Data is summarized in Table 2 for significant interactions. The data suggests that purine gene expression/dysregulation is related to the expression of specific inflammatory genes. Overall, in 9 of 17 purine genes that mRNA expression was up-regulated by LPS induction, there was a significant change in the slope of the linear relationship. For Adora2a, AMPD3, CD73, ENTPD2, and ENTPD3 there was an increase in slope for some genes and a decrease in slope for others. In contrast, for P2RX3, P2RX7, P2RY6, and P2RY1, there was a decrease in slope of the relationship. Therefore, a positive or negative interaction is revealed between purines and inflammatory genes depending on the specific purine gene. An additional analysis was done between Panx1, inflammatory, and purine genes. LPS induction decreased the slope of the linear relationship between mRNA expression of Panx1 and Caspase 3 or P2RX5.

Release of Mediators from hEGC Is Altered by LPS Treatment

Basal release of mediators was altered in hEGC treated for 24 hours with bacterial LPS and IFN-γ. Treatment increased basal release of the purinergic gliotransmitter ATP from hEGC ($P = 0.0017$) (Fig. 6A). In contrast, the same treatment with LPS and IFN-γ caused a significant reduction in s100β release ($P = 0.003$) (Fig. 6B).

LPS Alters Ca^{2+} Signaling, ATP-responses, Mechanosensitivity, and SOCE Responses

There was a clear and discrete change in flow-dependent mechanosensitivity. The flow-dependent (MS) activation of Ca^{2+} oscillations is dramatically reduced in hEGC treated with LPS, whereas cells are more likely to respond with Ca^{2+} oscillations under baseline/low flow stimulation. The proportion of cells responding to high flow was reduced by LPS treatment (Figs. 7 and 8).

Increase in the flow induces rhythmic Ca^{2+}oscillations in cells that do not have any baseline activity (Fig. 7A). Other cells can display Ca^{2+}oscillations at low flow (Fig. 7B). Increasing flow can alter the pattern of oscillations (Fig. 7B). Some cells display rhythmic Ca^{2+} oscillations at low flow and do not change their response with increase in flow (Fig. 7C). A variety of responses occur in response to low or high flow (Fig. 7A–F). Oscillations depend on extracellular Ca^{2+} levels (Fig. 7).

Restoring extracellular Ca^{2+} levels to 2 mM evokes a robust Ca^{2+} response (Fig. 7F, G). This is typical of activating store-operated Ca^{2+} channels and Ca^{2+} entry (SOCE) to refill the internal stores. ATP responses in these cells occur in the absence of extracellular Ca^{2+} ($0.0Ca^{2+}$ + EGTA buffer). Treatment with bacterial LPS alters/disrupts Ca^{2+} signaling, flow-dependent responses, ATP-induced Ca^{2+} transients, and SOCE responses in hEGC (Fig. 8G–L and Fig. 8).

DISCUSSION

A novel and important aspect of our study is identification of a molecular signature of the rhEGC phenotype in cells isolated and cultured from GI surgical specimens. Several steps in our isolation/culture protocol insured a yield of purified hEGC for nanostring analysis of gene expression. First, isolated ganglia composed of glia, neurons, and fibroblasts were the starting materials for growing hEGC cultures. Second, a 2-step purification process of hEGC by immune-isolation eliminates nonglial cells and results in a fairly pure population (98%–99%) of hEGCs in culture[7]; neurons do not survive in the culture medium used to grow hEGCs. Third, cells in purified hEGC cultures are virtually immune-positive for the glial marker s100β (99%), and lack staining for fibroblasts or smooth muscle cells.[7,10,11]

A custom nanostring panel of 107 genes proved to be a suitable readout in revealing the molecular identity of the rhEGC phenotype in response to inflammation. Bacterial lipopolysaccharide (LPS+IFN-γ) induced a "rhEGC phenotype" and caused an increase in mRNA expression of 58% of the genes, including 54% of inflammatory genes, several transcription factors, 52% of purine genes, 40% of ion channels, a majority of vesicular-transport proteins, free radical/antioxidant-genes, tight-junction proteins, certain postreceptor signaling pathways, and other proteins. In fact, the bacterial toxin highly discriminates between genes it targets for transcriptional regulation (i.e., among receptors, enzymes, channels, glial proteins, or tight junction

extracellular Ca^{2+} levels. Restoring extracellular Ca^{2+} levels to 2 mM evokes a robust Ca^{2+} response. This is typical of activating store-operated Ca^{2+} channels and Ca^{2+} entry (SOCE) to refill the internal stores. G, Example of a cell responding with a single Ca^{2+} transient to increase in flow and ATP response in 0.0 Ca^{2+} + EGTA. H, I, High flow responses are altered/disrupted after treatment. H–L, Treatment with bacterial LPS alters/disrupts Ca^{2+} signaling, flow-dependent responses, ATP-induced Ca^{2+} transients, and SOCE responses. Treatment alters flow-dependent responses, and typical responses seen in (A–F) are no longer evident. H and I, Flow-dependent responses are rare and rhythmic responses no longer occur. J–L, Other examples of abnormal Ca^{2+} responses characterized by lack of a normal flow-dependent response, small response to 0.0 Ca^{2+} and lack of sensitivity to ATP activation. Finally, the SOCE response is severely hampered (pooled data is in Fig. 8).

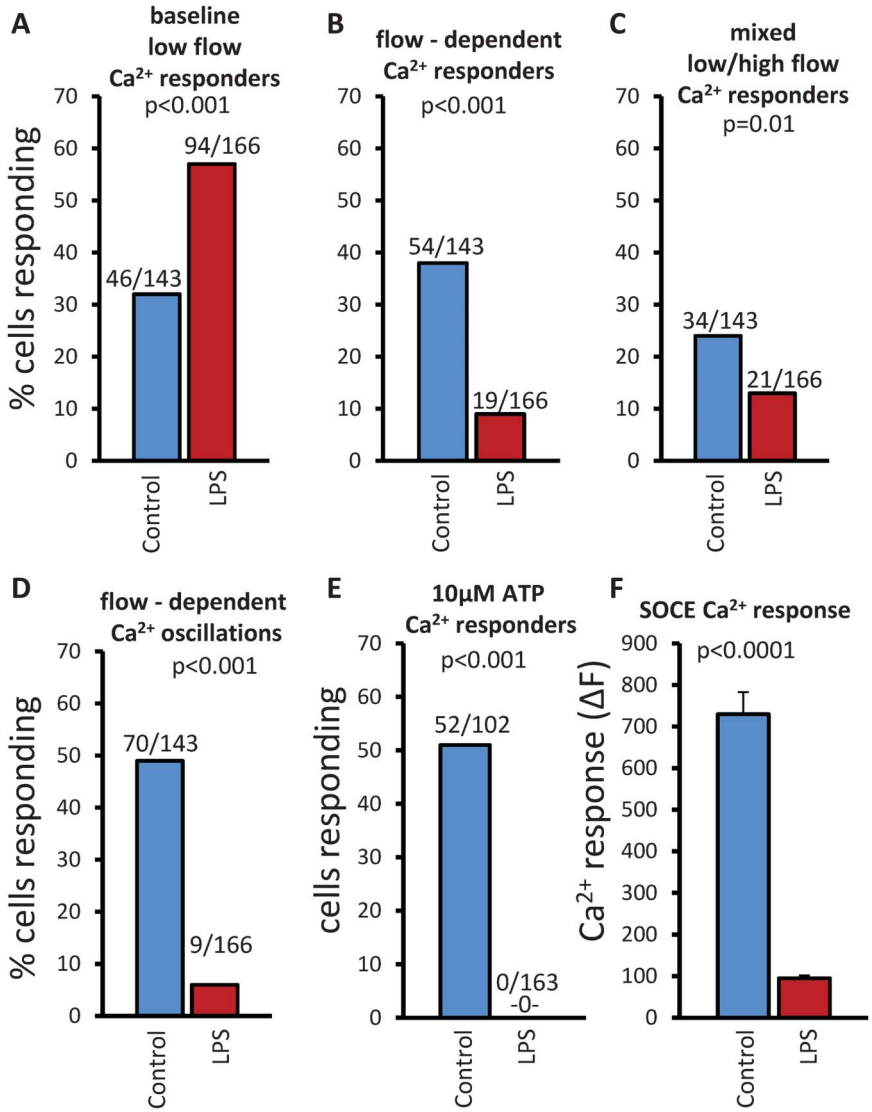

FIGURE 8. Bacterial LPS treatment alters and disrupts Ca^{2+} signaling and Ca^{2+} oscillations, mechanical activation of hEGC, ATP-induced Ca^{2+} responses and SOCE responses. A, After treatment, more cells are responsive to low flow with a Ca^{2+} response than in the absence of treatment. B, There is a dramatic reduction in flow-dependent Ca^{2+} responders. Therefore, treatment disrupts mechanosensitivity in hEGC. C, A reduction in low/high flow Ca^{2+} responders also occurs with treatment. D, Flow-dependent Ca^{2+} oscillations are nearly abolished by treatment. E, After treatment, cells are no longer sensitive to 10 μM ATP. It does not elicit a Ca^{2+} transient. F, SOCE Ca^{2+} responses are severely attenuated by treatment. Chi-square analysis was used to analyze data, and *P* values are shown. Numbers of cells responding are shown above the bars.

proteins in the same functional group). Therefore, a 15-fold increase occurs in mRNA expression of transient receptor potential channel TRPA1 whereas TRPV1 is only increased by 1.7-fold. The enzyme that regulates 5-HT metabolism, TPH2 is up-regulated 4.8-fold in hEGC, whereas mRNA expression of TPH1 (i.e., expressed in enterochromaffin cells) remains the same. The mRNA expression of the nicotinic channel CHRNA7 increased by 2.6-fold, whereas the toxin did not influence expression of several other channels (i.e., K^+ channel KCNE1, N-type Ca^{2+} channel CACNA1B, nicotinic channel CHRNA4). Also, mRNA expression of the glial s100B protein but not glial GFAP is up-regulated by bacterial toxin. The mRNA expression of one tight-junction protein CLDN1 was highly up-regulated by ~30-fold, whereas several others did not change. Treatment with LPS+IFN-γ had no effect on cell viability, and only a modest influence on apoptosis as indicated by a slight increase in mRNA expression of caspase-3.

In this study, we wanted to test the hypothesis that inflammation would cause significant alterations in purinergic signaling pathways in hEGC. Our data indicates that hEGCs express a full complement of purinergic receptors and enzymes needed for physiologic regulation of hEGC functions. Transcripts exist for all 29 purine genes including ATP-gated P2X channels ($P2X_2$, $P2X_3$, $P2X_4$, $P2X_5$, and $P2X_7$), metabotropic G-protein

TABLE 2. Significant Interactions Between Purine Genes and Inflammatory Genes

	Inflammatory Genes	
Purine Gene	Increase in Slope "m"[a]	Decrease in Slope "m"[b]
Adora2a	IL-6,[c] IL-8, GATA_3, CLDN1	C3
AMPD3	SOCS3[c]	CCL2,[c] IP10, IL-4, IL-8
NT5E/CD73	STAT3,[c] GATA3	C3, IL-33
ENTPD2	IL-6, IL-8, GATA3, CLDN1, CCL3	C3
ENTPD3	GATA_3, IP10	GMCSF
P2XR3		C3
P2RX7		CCL2, IL-12_A, IL-17A, IL-4, IL-6, IL-8, IP10
P2RY6		CCL2, GATA_3, IL-17A, IL-4, IL-8, IP10
P2RY1		C3, IL-4
Related gene		
Panx1		*CASP3, P2XR5*

[a]Significant increase in the slope of the linear relationship plotted between the inflammatory gene (X_1) versus the purine gene (Y_1) ($P < 0.01$ denotes significant differences in slope "m" of line $Y_1 = m_1X_1 + B_1$).
[b]Significant decrease in the slope of the linear relationship plotted between the inflammatory gene (X_2) versus the purine gene (Y_2) ($P < 0.01$ denotes significant differences in slope "m" of line $Y_2 = m_2X_2 + B_2$).
[c]Significant interactions.

coupled P2Y receptors ($P2Y_1$, $P2Y_2$, $P2Y_4$, $P2Y_6$, $P2Y_{11}$, $P2Y_{12}$, $P2Y_{13}$, and $P2Y_{14}$), adenosine receptors (A_1, A_{2a}, A_{2b}, and A_3), as well as enzymes involved in the metabolism of endogenous nucleotides, nucleosides, and di-nucleotides. These enzymes include adenosine monophosphate (AMP)/ADA enzymes (AMPD3, AMPD2, ADA1, and ADA2), ectonucleoside triphosphate diphosphohydrolases (ENTPD1, CD39; ENTPD2, and ENTPD3), nicotinamide enzymes (NADSYN1, NMRK1, and NMNAT1), NT5E (CD73), and DDP4. The highest constitutive expression of mRNA for purine genes is for DDP4, CD73, AMPD3, NMRK1, NMNAT1, P2RX5, and P2RY11; in the inflamed state, mRNA expression of only AMPD3 was increased, and hence the other 6 highly expressed purine genes are not regulated by inflammation.

LPS induction caused selective up-regulation in mRNA expression of subsets of receptors and enzymes in hEGC. Therefore, 9/17 (53%) receptors and 6/13 (46%) enzymes were regulated by inflammation. The order of highest to lowest up-regulation was Adora2a (27-fold) > AMPD3 (8.3-fold) > $P2RY_{13}$ (6-fold) > P2RY2 (4.3-fold) > P2RX3, P2RX7 (4-fold) > P2RY1, P2RY14, P2RY6, ENTPD2, ENTPD3 (3-fold) > NADSYN1 (2-fold) > Adora2b (1.7-fold). From previous studies, purinergic signaling pathways are known to be sensitive to inflammation and changes in purinergic gene expression occurs for receptors and enzymes in purinergic pathways in response to gut inflammation.[14–17] This study revealed for the first time that purine gene dysregulation is an important mechanism in the rhEGC phenotype.

Our data support the novel hypothesis that bacterial toxin (or inflammation) induces a phenotypic switch from ATP signaling to other forms of purinergic signaling. The supporting arguments are briefly discussed. First of all, AMPD3 (and ENTPD3 to a lesser extend) is up-regulated favoring the breakdown of ATP. Secondly, the PDE4B/cAMP/CD73 adenosinergic pathway is facilitated by bacterial toxin. For instance, PDE4B, the enzyme for breaking down cAMP to AMP is up-regulated, whereas protein kinase A, the target enzyme for cAMP is down-regulated. This favors a pathway towards AMP and adenosine production. In fact, as noted, the mRNA expression of CD73 (NT5E) is not altered by inflammation but this enzyme has the highest constitutive expression of mRNA among 29 purine genes analyzed. This is significant because CD73 is a membrane-bound enzyme in the PDE4B/cAMP/CD73 adenosinergic pathway that converts AMP produced from cAMP, release from the cells to adenosine. Adenosine activates A_{2a} and to a lesser extent A2b receptors. A_{2a} expression is up-regulated by 27-fold in response to bacterial toxin, $A_{2b}R$ is modestly up-regulated and A_1/A_3 are not affected. ADA (2 isoforms, ADA1/ADA2) that inactivates adenosine or DDP4 that inhibits ADA is not affected by treatment. The mRNA counts for both CD73 and DPP4 are very high in hEGC compared with other purine genes. Therefore, conservation of expression of these genes would insure that adenosinergic signaling is spared by LPS induction. There is also a 8.3-fold up regulation of mRNA levels of AMPD3. AMPD3 converts ATP to ADP to AMP and adenosine. Specifically, data are consistent with facilitation of the cAMP (PDE4/PKACA)-dependent adenosinergic A_{2A} pathway and relevant pathway enzymes (AMPD3/ENTPD2/DDP4/ADA1 and ADA2). Finally, ATP-dependent functional signaling is disrupted in hEGC by treatment. The stimulatory effect of exogenous ATP on Ca^{2+} responses in hEGC is mitigated by bacterial toxin treatment, even in the presence of higher basal release of ATP in response to treatment.

The mRNA expression of CD39 (ENTPD1), an ectonucleoside triphosphate diphosphohydrolase is not altered in hEGC. ENTPD2 and ENTPD3 are up-regulated by LPS+IFN-γ in hEGC. Up-regulation of $P2Y_1$ and $P2Y_{13}$ receptors favors ADP signaling in hEGC, whereas the up-regulation of $P2Y_2$ and $P2Y_6$ receptors favors UTP signaling. Taken together, our data support the novel hypothesis that bacterial LPS induces a phenotypic switch from nucleotide/ATP to ADP signaling ($P2Y_1/P2Y_{13}$), adenosinergic signaling (A_{2a}/A_{2b}), and UTP signaling ($P2Y_2/P2Y_6$) in the rhEGC phenotype that will likely disrupt glial physiology, because purines are important regulators of Ca^{2+} signaling in hEGCs.[11,18] Mechanistic studies can test this hypothesis.

The ectoenzymes ectonucleoside triphosphate diphosphohydrolase (CD39) and ecto-5′nucleotidase (CD73) regulate breakdown of ATP and ADP to AMP and conversion of AMP to

adenosine, respectively. This adenosine mechanism is important in protecting against development of inflammation.[19–21] Both A_{2a} and A_{2b} could be involved in protection. Methotrexate and sulfasalazine are drugs used to treat IBD, and their mechanism of action is in part via enhanced release of extracellular adenosine via a CD73-dependent mechanism.[21,22] Dipyridamole is a nucleoside uptake inhibitor, and by elevating extracellular levels of adenosine, it is effective in suppressing the inflammatory response in experimental human endotoxemia. In Chagas disease (i.e., infection with *Trypanosoma cruzi*), CD39 is reduced in lymphocytes of patients with the disease.[23]

In human colon, glia outnumber neurons 7 to 1,[24,25] suggesting a more prominent role of glia in human than rodent ENS, where up-regulation of ectonucleotidases can be a critical neuroprotective mechanism, to limit neuronal cell death through release of large amounts of ATP from cell lysis acting on the cytotoxic $P2X_7$/Panx1 receptor pathway in neurons. Glial cells play a similar role with glutamate,[26] and uptake of glutamate by glia prevents high extracellular levels that could potentially be neurotoxic.

In astrocytes, LPS was shown to enhance ATP hydrolyzing activity by different mechanisms. IFN-γ decreases the relative abundance of NTPDase2[27] and changes the nucleotide phosphodiesterase (NTPDase) ratio towards NTPDase1, which contributes to formation of adenosine (to act on P1 receptors). In contrast LPS up-regulates NTPDase2 and contributes to accumulation of ADP and activation of P2Y receptors. NTPDase2 converts ATP to ADP ($P2Y_1$, $P2Y_{12}$, and $P2Y_{13}$), and NTPDase1 bypasses the formation of ADP and forms adenosine (P1).[28] We did not test LPS and IFN-γ separately in hEGC to evaluate stimulus-specific modulation of NTPDases expression. In rodent colon, neurons express NTPDase 3 and enteric glial cells express NTPDase2.[29] NTPDase2 is the dominant ectonucleotidase expressed in rat astrocytes as well.[27] We found mRNA expression of all 3 ecto-5′nucleotidases in hEGC, and the expression of NTPDase 2 and 3 is modulated by inflammation. High NTPDase 2 and NTPDase 3 activity in the LPS-induced rhEGC phenotype may provide a protective mechanism for glia and neurons from high levels of extracellular ATP that can cause neurotoxicity and neuronal cell death, as shown for IBD[30] or in vitro model of ischemia,[31] cell cultures, or organotypic culture.[32] A shift to ADP/adenosine is presumed to be neuroprotective by suppressing neuronal excitability through inhibitory A_1/A_3 sites in human ENS. In the central nervous system, astrocytes are the main source of extracellular nucleotides, and important regulatory enzymes exist for control of external concentration of nucleotides. Ectonucleotidases constitute a complex enzymatic cascade to regulate nucleotide signaling, controlling rate, amount and timing of nucleotide degradation, and nucleoside/adenosine formation. Alterations in expression of these enzymes may disrupt hEGC physiology.

Metabotropic P2Y receptors that are up-regulated are $P2Y_1$, $P2Y_2$, $P2Y_6$, $P2Y_{13}$, and $P2Y_{14}$. The endogenous ligands for these receptors are ADP for $P2Y_1$ and $P2Y_{13}$, UTP for $P2Y_2$ and $P2Y_6$, and uridine diphosphate-glucose for $P2Y_{14}$.[13] Among nucleotides, our previous study showed that UTP activates more hEGCs than ATP or other agonists,[10,11] and therefore UTP responses in addition to adenosine responses may play a more prominent role in the rhEGC phenotype. In other studies in the past, inflammation was shown to alter enteric glial cell expression of mGluR5[33] and endothelin receptors in animals.[34] These possibilities will be explored in future studies.

The $P2Y_{13}$ receptor is involved in apoptosis of neurons in the ENS, and neurons of the ENS in $P2Y_{13}$ receptor null mice are resistant against high fat diet and palmitic acid–induced neuronal loss.[35] Our study identified for the first time mRNA expression of $P2Y_{13}$ in hEGC, and expression is ~6-fold up-regulated by bacterial LPSs. The $P2Y_{13}$ receptor is a target of interest in GI inflammatory disorders for apoptosis/neuroprotection. Overall, A_{2a}, AMPD3, $P2Y_{13}$, $P2Y_2$, $P2X_3$, and $P2X_7$ are novel purinergic targets in the rhEGC phenotype, and their level of up-regulation (4–27-fold) is expected to cause abnormal purinergic Ca^{2+} signaling, Ca^{2+} waves, and glial modulation of neural and motor behavior.[12]

Preliminary data show that basal secretion of ATP, ADP, AMP, ADO, and NAD occurs in hEGC,[10] and enzymes exist for degradation of the endogenous ligands. Remarkably, basal release of ATP was increased 5-fold by LPS induction, whereas s100B release was reduced by induction in hEGC. The mechanism is not known, but what is known is that inflammation, and specifically IL-1β and TNF-α can cause opening of hemichannels in glia that can release large molecules such as ATP, glutamate or others, which can kill neurons in co-culture through activation of pannexin hemichannels (Panx1). The mRNA levels of these proinflammatory cytokines were up-regulated in hEGC in response to LPS induction, and hemichannels could potentially be involved. Panx1 is also up-regulated in hEGC, and it may be important in human glial pathophysiology as in astrocytes.[36] Whether other hemichannels are expressed or up-regulated with inflammation is not known in hEGC. But, we now know that multiple hemichannels may be involved in cell-to-cell communication in hEGC and may include connexins and pannexins.[10] Another possibility is that up-regulation of vesicular transport proteins facilitates basal ATP release in hEGC. The mRNA expression of 3 proteins (SYT2, SNAP25, and SYP) was increased 3.6 to 6-fold by bacterial toxin. SYT2, synaptosomal associated protein SNAP25 and synaptophysin are up-regulated, suggesting a role in gliotransmission in inflamed states. The functional roles of purinergic signaling pathways in normal and inflamed states of hEGC await further investigation.

Our recent preliminary studies showed that hEGC is a useful model to study glial function.[10,11] MS plays a key role in the physiology of hEGC–they trigger Ca^{2+} oscillations and Ca^{2+} waves in hEGC. In this study, we found that there is clear and discrete change in flow-dependent activation of hEGC that triggers Ca^{2+} oscillations. After bacterial toxin treatment, hEGC change their behavior by being less responsive to MS. Treatment increased sensitivity of cells at low flow and almost prevented flow-dependent Ca^{2+} responses. We propose that such a Δ mechanosensitivity will alter the ability of hEGC to respond to MS

(i.e., muscle contractions, increase in intraluminal pressure, distension, and stretch or deformation of glial membranes) associated with various physiologic motor patterns (i.e., peristalsis, propulsion, colonic migrating motor complexes, mass movement/evacuation reflex during defecation, the migrating motor complex (MMC), or mixing movements during the digestive phase). LPS further disrupts Ca^{2+} dynamics, as indicated by a severely diminished SOCE Ca^{2+} response. In addition, the Ca^{2+} response induced by ATP is severely disrupted as noted earlier. MS is known to trigger release of purines like ATP in most cells.[17,37] We propose that a Δ mechanosensitivity in hEGC would contribute to abnormal neuromuscular function and motility by disrupting Ca^{2+} and purinergic signaling, because MS and ATP trigger both Ca^{2+} oscillations and Ca^{2+} waves in glia, events that are linked to motility.[2,12] Another contributing factor is a shift in purinergic signaling from ATP to ADP, UTP, and adenosinergic signaling as indicated by changes in molecular signaling of purinergic pathways.

The NFkB signaling transcription pathway is an important pro-inflammatory pathway in EGC that contributes to harmful effects of the reactive glial phenotype. In hEGC, NFkB signaling is involved in the TLR/RAGE/s100B–dependent iNOS/NO signaling pathway induced by LPS or pathogenic bacteria[7] and ulcerative colitis in humans,[38] as well as DSS colitis in mice.[8,39,40] STAT3 (signal transducer and activator of transcription 3) and SOCS3 (suppressor of cytokine signaling 3) are involved in negative regulation of cytokines and their expression in hEGC was increased in response to LPS. STAT3 is known to suppress pro-inflammatory signaling mechanisms in astrocytes.[41] The mRNA counts/sample for STAT3 was the highest for all transcription factors (i.e., >1000 mRNA counts versus ≤50 mRNA counts/100 ng RNA sample for 6 other transcription factors), and its expression increased in response to LPS. This suggests an important role in the physiology of EGC and in dampening inflammatory responses in hEGC. FOXP3 is up-regulated by 4.5-fold. FOXP3 is a master regulator/transcription factor involved in immune responses, development and function of regulatory T cells. Deficiency is associated with multi-organ autoimmunity in Scurfy mutant mice and human patients with enteropathy and other syndromes.[42] Our study extends our knowledge, and provides evidence that the transcription factors RelB, RelA, SOCS3, FOXP3, GATA_3, and aryl hydrocarbon receptor are up-regulated by LPS–. Overall, the net effect of transcriptional regulation is to induce a detrimental rhEGC phenotype.

Toll-like receptors (TLRs) are receptors that mediate innate immune responses in astrocytes and EGC. TLRs recognize LPS (a membrane component of Gram-negative bacteria) such as *Enteroinvasive E. coli*. Bacterial LPS activates multiple TLRs in hEGC,[7] and it is likely that not all changes in the rhEGC phenotype are the result of a single TLR activation. TLR4 activation causes NO production through an s100B/RAGE/iNOS mechanism. In this study, the TLR signaling mechanisms linked to gene dysregulation in the rhEGC is unknown. In astrocytes TLR3 signaling induces the strongest pro-inflammatory response involving secretion of high levels of IL-12, TNF-α, IL-6, CXCL-10 (IP10), and IL-10.[43] CCL2, CCL5, 7, 8, 12 are also activated in astrocytes in response to LPS.[41] In hEGC, TLR4 signaling involves MyD88/RAGE/s100B-iNOS/NO signaling pathway through NFkB signaling.[7] Palmitoylethanolamide exerts its anti-inflammatory effects by targeting the s100B/TLR4 dependent peroxisome proliferator-activated receptors α activation on EGC, causing a downstream inhibition of NFkB-dependent colonic inflammation.[8] Our study identified many new signaling pathways linked to global activation of TLRs in hEGC by LPS. Highly regulated genes included both chemokines and cytokines, but the response was overwhelmingly pro-inflammatory or detrimental, although a few anti-inflammatory genes were also increased with LPS. Pro-inflammatory chemokine up-regulation of expression from highest to lowest was in the order of IP10 (CXCL-10) >> Cxcl2 = CCL3 > CCL2 (MCP-1) > s100B; s100B is proposed to represent a marker of the severity of inflammation in ulcerative colitis,[6,7] and is implicated in TLR signaling in response to LPS or *E. coli* infection in hEGC.[7] At least in hEGC, much stronger up-regulation occurs for 4 other chemokines (e.g., s100B increased by 3-fold versus Cxcl2 of greater than 1000-fold and CCL3 [150-fold], CCL2 [MCP1, 12-fold] and IP10 [CXCL-10, > 10,000-fold], v. low basal levels). Their mechanism of action is not known. Pro-inflammatory cytokine genes that were strongly up-regulated included from high to low IL-8 > IL-6, IL-1β, TNF-α, IL-4 > IL-23A, IL-33, IL-17A, IL-12A, and IL-2R. Among the cytokines, IL-10 and IL-22 are the only anti-inflammatory cytokines.[44–46] that displayed up-regulation (5–7-fold) in hEGC. Expression of transforming growth factor beta 1 did not change with LPS. Neutralizing antibodies have shown the therapeutic potential of IL-23 and IL-12 in experimental colitis and clinical trials of IBD, specifically in patients with CD resistant to TNF-α therapy.[47,48] In hEGC, up-regulation of IL-23A (20-fold) is much greater than IL-12 (5-fold). It is tempting to speculate that hEGC is one of the cellular targets for the beneficial effects of antibody therapy in CD, especially since *E. coli* bacterial infection is a prominent feature in ~36% of CD patients with ileal involvement,[49] and these responses are likely to occur in hEGC in these patients. Various cytokines and chemokines released by reactive hEGC could potentially have a profound effect on surrounding cells in the gut including other glia in the networks, immune cells, neurons, interstitial cells of Cajal (ICC), enteroendocrine cells and epithelial cells.

TLR2 signaling regulates intestinal inflammation in a protective manner by controlling ENS structure neurochemical coding, as well as neuromuscular function. These data provide some insight as to how TLR2 signaling in the ENS may affect the IBD phenotype in humans.[50] LPS also enhanced the action of bradykinin in the ENS by secretion of IL-1β from rat EGCs.[51] LPS/cytokines stimulate release of NO, IL-1β, IL-6, and PGE2 from rodent EGC.[52] The current study in hEGC identified the nature of the pro-inflammatory response to LPS that can directly contribute to intestinal inflammation. IL-1β expression was up-regulated 25-fold in hEGC. IL-1β signaling in EGC was shown to be involved in POI in the mouse.[9] IL-1β also attenuates EGC

proliferation whereas LPS and IFN-γ together stimulate glial cell proliferation.[37] We identified a large number of pro-inflammatory genes that are regulated by LPS induction.

Inflammatory cytokines modify intracellular free Ca^{2+} levels in EGC and regulate expression of glial proteins GFAP and s100B, and these responses are pro-inflammatory and detrimental.[7,9,51] In our study of hEGC, LPS increased s100B but not GFAP mRNA expression. In vivo intestinal inflammation stimulates proliferation of myenteric EGC.[53] NO contributes to pro-inflammatory reactions.

T_H1 associated cytokines are IFN-γ and IL-2, and in the presence of LPS, their expression levels were increased by 5 to 6-fold. TH2-type cytokines include IL-5, IL-4, and IL-13 associated with transcription factor GATA3.[54] Only IL-4 expression increased by LPS, but the increase was 20-fold. Therefore, Th1 and Th2 associated cytokine genes are altered in different ways in hEGC.

EGC may exert a neuroprotective role for enteric neurons from oxidative stress–induced cell death and increase neuronal survival in part by reduced glutathione.[55] The glial mediators glutathione, glial cell line-derived neurotophic factor (GDNF) and 15dPGJ2 exert neuroprotective effects.[55,56] In astrocytes, up-regulation of SOD2 and catalase attenuates oxidative stress.[57] Astrocyte depletion impairs redox homeostasis and triggers neuronal loss in the adult central nervous system; neutralization of reactive oxygen species and reactive nitrogen species protects against neural injury.[58] Earlier reports suggested that neurons depend on antioxidant potential of astrocytes for their own defense against oxidative stress in vitro.[59] There is critical involvement of astrocytes in redox homeostasis and lesioning of astrocytes in vivo leads to oxidative stress and neuronal decline. From a translational viewpoint, neuroprotective interventions might be more likely to succeed if they target metabolic integrity of the glia-neuron interface. It is highly significant therefore, that in hEGC, mRNA expression of SOD2 is up-regulated by 45-fold in response to LPS. It inactivates highly reactive superoxide free radicals and converts O_2^- to hydrogen peroxide. It is a signal that free radicals are elevated in the rhEGC. This is a novel protective mechanism that may provide glial and neuronal protection in an effort to preserve the normal neural-glial environment in human ENS. Free radicals increase the permeability of Cx43 hemichannels to large molecules or their open probability[60] and they are involved in Ca^{2+} waves in hEGC.[10]

A novel finding is that HMOX1 mRNA level is increased by 2-fold in hEGC in response to LPS. The heme-degrading enzyme HMOX1 promotes iron deposition, mitochondrial damage, and autophagy in astrocytes and enhances vulnerability of neurons to oxidative stress/injury. It is suggested that in chronic central nervous system disorders, over-expression of glial HMOX1 may contribute to neural damage.[61] This may have implications for GI disorders with ENS dysfunction. The inducible NO synthase enzyme (NOS2) is also up-regulated in hEGC by 6-fold. Increase in NO production has been shown to involve a TLR/RAGE/s100B–iNOS/NO pathway in hEGC.[7] Increased production of NOS2 in enteric glia contributes to dysregulation of intestinal ion transport in mice with colitis. Blocking EGC function restores epithelial barrier function and also decreases bacterial translocation.[39]

Data analysis suggested that significant interactions exist between purine genes and inflammatory genes (i.e., a change is slope of the linear relationship between mRNA expression of specific purine genes and inflammatory genes). A positive or negative interaction is revealed between purines and inflammatory genes depending on the specific purine gene. This supports the hypothesis that expression of specific purine genes is regulated by different mechanisms. It is likely that complex interactions exist between inflammation and purinergic signaling pathways and that specific inflammatory mediators generated by LPS-induction of hEGC (or gut bacterial infection) differentially modulate purine gene expression. This provides a short list of purine genes (9 of 29) and candidate inflammatory targets for testing it in future studies.

A working model of the molecular signaling pathways activated in the rhEGC phenotype is illustrated in Figure 9. Our findings provide significant new insights into the molecular mechanisms and pathophysiology of the rhEGC phenotype. Discrete up-regulation of mRNA expression levels occurred in certain genes. Major molecular pathways of dysregulation include inflammatory mediators, growth factors, transcription factors, purine genes, vesicular transport proteins, free radical pathways, angiotensin receptors, TRP channels, Panx1 hemichannels, enzymes for metabolism of 5-HT, purine nucleosides, nucleotides and di-nucleotides, a barrier protein CLDN1 and cAMP-dependent pathways PDE4/PKACA. As shown in Fig. 9A, our working hypothesis is that LPS induction (or bacterial infection) activates TLRs leading to transcriptional regulation (via SOCS3/STAT3/GATA_3/RELA/RELB) and up-regulation of inflammatory genes (including cytokines, chemokines and growth factors). Inflammatory mediators and transcription factors work in concert to cause dysregulation/up-regulation in gene expression profiles of selected clusters of purine genes, TRP channels, neurotransmitters/signaling, vesicular transport proteins, second messengers, junction/barrier proteins, and free radical pathways. The receptors and molecular signaling pathways affected by bacterial LPS are illustrated in Fig. 9B. Bacterial LPS induction disrupted glial function and altered mechanosensitivity, ATP Ca^{2+} responses, ATP (and s100B) release, and Ca^{2+} handling mechanisms (i.e., SOCE response). Changes in these molecular signaling pathways in response to inflammation would disrupt motility and intestinal transit. Overall, specific changes in the rhEGC phenotype include (1) ΔCa^{2+} signaling, (2) Δ purinergic signaling, (3) ΔPanx1 hemichannels, (4) switch from ATP to ADO/ADP/UTP signaling, (5) Δ vesicular transport proteins that may facilitate release of ATP, (6) Δ transmitter signaling, (7) Δ Sensory signaling, (8) Δ free radical/antioxidant pathways, (9) Δ Ca^{2+} waves[10,11] and (10) a Δ in receptor expression.

This study identified a large piece of the puzzle related to the rhEGC phenotype activated by bacterial toxin. The ENS is affected in patients with neurological and GI disorders (slow transit constipation, irritable bowel syndrome, motility, Chagastic megacolon). Some of the highly regulated genes in hEGC may have implications for IBD, and in particular CD for which data suggest that bacteria play a role in the onset and propagation of

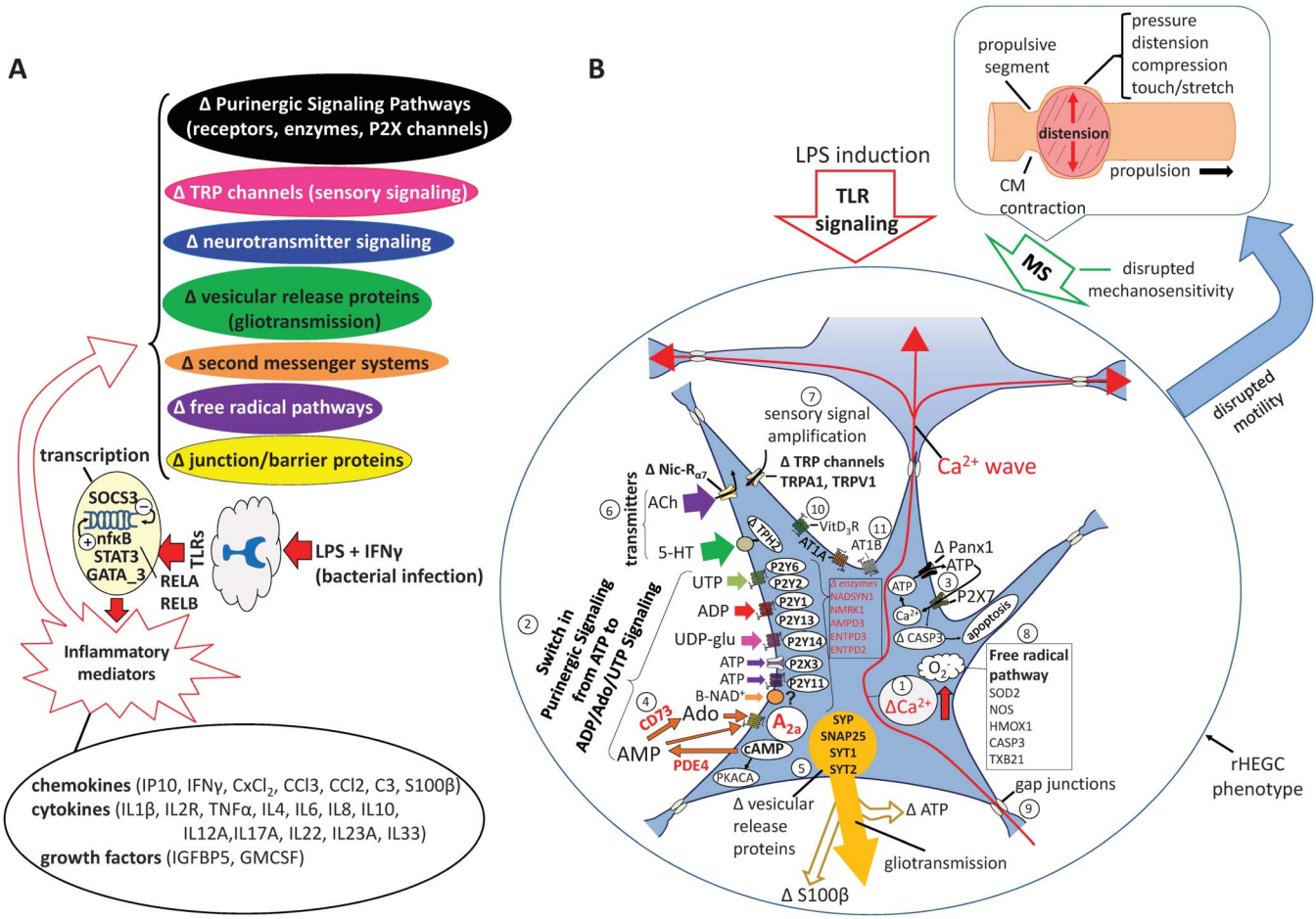

FIGURE 9. A working hypothesis of the molecular signaling pathways activated in the rhEGC phenotype in response to bacterial LPS activation. Gene expression was altered in 58% of genes (107 genes) including 54% of inflammatory genes, 52% of purine genes (15 of 29 genes), 40% of channels, vesicular transport proteins, transcription factors, free radical pathways, second messenger systems, and other proteins. Ninety-five percent of genes were up-regulated by treatment. A, Our working hypothesis is that LPS induction (or bacterial infection) activates TLRs leading to transcriptional regulation (via SOCS3/STAT3/GATA_3/RELA/RELB) and up-regulation of inflammatory genes (including cytokines, chemokines and growth factors). Inflammatory mediators and transcription factors work in concert to cause dysregulation/up-regulation in gene expression profiles of selected clusters of purine genes, TRP channels, neurotransmitters/signaling, vesicular transport proteins, second messengers, junction/barrier proteins, and free radical pathways. The receptors and molecular signaling pathways are affected by bacterial LPS (B). Overall disruption in glial molecular signaling pathways is likely to contribute to abnormal Ca^{2+} waves, gliotransmission, purinergic signaling, and mechanosensitivity. Propulsion and flow of contents in the lumen of the intestinal tract occurs as a result of oral CM contraction in the propulsive/oral segment and distal relaxation in the receiving segment to allow flow/movement of luminal contents. Mechanical forces generated during peristalsis (Δ intraluminal pressure, compression forces, tactile stimulation, Δ flow, CM contraction, or the peristaltic wave) can trigger Ca^{2+} waves in hEGC to modulate ENS activity and motor behavior. Purinergic signaling also triggers Ca^{2+} waves in hEGC. Changes in these molecular signaling pathways in response to inflammation would disrupt motility and intestinal transit. Specific changes in the rhEGC phenotype include (1) Δ Ca^{2+} signaling, (2) Δ purinergic signaling, (3) ΔPanx1 hemichannels, (4) switch from ATP to Ado/ADP/UTP signaling, (5) Δ vesicular transport proteins that may facilitate release of ATP, (6) Δ transmitter signaling, (7) Δ sensory signaling, (8) Δ free radical/antioxidant pathway, (9) Δ Ca^{2+} waves, and (10) a Δ in receptor expression. A rhEGC and those genes and pathways represent new targets of investigation in diseases involving infection, intestinal inflammation, neurologic disorders, and GI disorders.

IBD. Invasive *E. coli* is restricted to CD, and is isolated from ileal biopsies of 36% of CD patients with ileal involvement. The pathogenesis of CD is postulated to be closely linked to the presence of invasive *E. coli*. In IBD, dysbiosis may induce a breakdown in the balance between "putative species of harmful (i.e., adherent-invasive *E. coli*) and protective bacteria" (*Bifidobacterium* & *Lactobacillus* species) (48). The influence of other products (e.g., flagellin) and invasive bacteria such as *Shigella flexneri*, enterotoxinogenic *E. coli*, *Listeria monocytogenes*, and *Yersinia enterocolitica* on hEGC remains unknown.

The molecular phenotype represents many novel potential therapeutic targets of investigation in hEGC for treating motility

disorders (and slow transit constipation),[12] GI disorders,[1] IBD,[62] POI,[9] and infectious diseases.[7] Both animal studies[2,3] and human in vitro studies strongly support the concept that EGCs are involved in the modulation of motor function in the intestinal tract.[12] Inflammation may change the overall pattern of purinergic signaling by causing up-regulation in 9 receptor genes (A_{2a}, $P2Y_{13}$, $P2Y_2$, $P2X_3$, $P2X_7$, $P2Y_1$, $P2Y_{14}$, $P2Y_6$, and A_{2b}) and 6 purinergic enzymes (AMPD3, ENTPD3, ENTPD2, NADSYN1, etc). Our study tested a single inflammatory stimulus, but the molecular phenotype may depend on the type of stress or injury,[63] and the type of inflammatory stimulus, severity or chronicity of inflammation is also likely to have an impact on the molecular phenotype. Reactive hEGC induced by LPS exhibited a pro-inflammatory phenotype that was overwhelmingly detrimental, although several protective genes were up-regulated (i.e., IL-10, IL-22, SOD2, SOCS3, STAT3, Wnt-β-catenin signaling, and adenosinergic pathways). The importance of studies in EGC is highlighted by the fact that EGCs represent a transcriptionally unique population of glia in the mammalian nervous system.[65]

ACKNOWLEDGMENTS

Supported by Diabetes and Kidney Diseases R01 DK093499 and Strategic initiative funds from the Department of Anesthesiology to F. L. Christofi toward developing a Neuromodulation Program. F. Turco was a visiting scholar in Dr. Christof's Purine Neuromodulation Lab from R. Cuomo's group at the University of Naples, Italy. This work was also supported by a grant to F. Turco and R. Cuomo from the Italian Ministry of University and Research, COFIN project 2009HLNNRL; E. Whitaker is a physician scientist in Dr. Christofi's lab supported by an NIH Loan Repayment Grant and a pre-K NIH CTSA Award; Genomics Core Lab services were used for RNA quality measurement and NanoString data generation; Peter Vaccarella created the artwork and illustrations. The remaining authors have no conflict of interest to disclose.

Author contributions: Study design, scientific conduct of the study, data collection and analysis, interpretation, and/or writing of the manuscript, A. Liñán-Rico, F. Turco, F. Ochoa-Cortes, I. Grants, E. Whitaker, M. Abdel-Rasoul, B. J. Needleman, A. Harzman, R. Arsenescu, R. Cuomo, P. Fadda, and F. L. Christofi; B. J. Needleman, and A. Harzman *were the GI surgeons coordinating the effort to procure viable GI surgical specimens from nondiseased bowel to prepare hEGC cultures*; F. Turco, A. Liñán-Rico, F. Ochoa-Cortes, and I. Grants *developed and standardized hEGC cultures for functional studies*; A. Liñán-Rico, F. L. Christofi, and R. Arsenescu *designed the gene set for nanostring analysis*; A. Liñán-Rico *conducted Ca^{2+} and release experiments*; M. Abdel-Rasoul *was involved in the biostatistical analysis and interpretation*; P. Fadda *conducted the nanostring analysis.*

REFERENCES

1. Fujikawa Y, Tominaga K, Tanaka F, et al. Enteric glial cells are associated with stress-induced colonic hyper-contraction in maternally separated rats. *Neurogastroenterol Motil.* 2015;27:1010–1023.
2. McClain JL, Grubišić V, Fried D, et al. Ca^{2+} responses in enteric glia are mediated by connexin-43 hemichannels and modulate colonic transit in mice. *Gastroenterology*. 2014;146:497–507.
3. Nasser Y, Fernandez E, Keenan CM, et al. Role of enteric glia in intestinal physiology: effects of the gliotoxin fluorocitrate on motor and secretory function. *Am J Physiol Gastrointest Liver Physiol.* 2006;291:G912–G927.
4. Sharkey KA. Emerging roles for enteric glia in gastrointestinal disorders. *J Clin Invest.* 2015;125:918–925.
5. Cornet A, Savidge TC, Cabarrocas J, et al. Enterocolitis induced by autoimmune targeting of enteric glial cells: a possible mechanism in Crohn's disease? *Proc Natl Acad Sci U S A.* 2001;98:13306–13311.
6. Ochoa-Cortes F, Turco F, Liñán-Rico A, et al. Enteric glial cells: a new frontier in neurogastroenterology and clinical target for Inflammatory Bowel Diseases. *Inflamm Bowel Dis.* 2016;22:433–449.
7. Turco F, Sarnelli G, Cirillo C, et al. Enteroglial-derived S100B protein integrates bacteria-induced Toll-like receptor signalling in human enteric glial cells. *Gut*. 2014;63:105–115.
8. Esposito G, Capoccia E, Turco F, et al. Palmitoylethanolamide improves colon inflammation through an enteric glia/toll like receptor 4-dependent PPAR-α activation. *Gut*. 2014;63:1300–1312.
9. Stoffels B, Hupa KJ, Snoek SA, et al. Postoperative ileus involves interleukin-1 receptor signaling in enteric glia. *Gastroenterology*. 2014; 146:176–187.
10. Ochoa-Cortes F, Linan-Rico A, Zuleta-Alarcon A, et al. Mechanosensory signaling in human enteric glial cells. *Gastroenterology*. 2016;150:S345.
11. Liñán-Rico A, Ochoa-Cortes F, Zuleta-Alarcon A, et al. Modulation of Ca^{2+} waves in human enteric glial cells. *Gastroenterology*. 2015;148:S-79.
12. Liñán-Rico A, Grants I, Needleman BJ, et al. Gliomodulation of neuronal and motor behavior in the human GI tract. *Gastroenterology*. 2015;148:S-18.
13. Ochoa-Cortes F, Liñán-Rico A, Jacobson KA, et al. Potential for developing purinergic drugs for gastrointestinal diseases. *Inflamm Bowel Dis.* 2014;20:1259–1287.
14. Guzman J, Yu JG, Suntres Z, et al. ADOA3R as a therapeutic target in experimental colitis: proof by validated high-density oligonucleotide microarray analysis. *Inflamm Bowel Dis.* 2006;12:766–789.
15. Rybaczyk L, Rozmiarek A, Circle K, et al. New bioinformatics approach to analyze gene expressions and signaling pathways reveals unique purine gene dysregulation profiles that distinguish between CD and UC. *Inflamm Bowel Dis.* 2009;15:971–984.
16. Ren T, Grants I, Alhaj M, et al. Impact of disrupting adenosine A_3 receptors ($A_3^{-/-}$ AR) on colonic motility or progression of colitis in the mouse. *Inflamm Bowel Dis.* 2011;17:1698–1713.
17. Liñán-Rico A, Wunderlich JE, Grants IS, et al. Purinergic autocrine regulation of mechanosensitivity and serotonin release in a human EC model: ATP-gated P2X3 channels in EC are downregulated in ulcerative colitis. *Inflamm Bowel Dis.* 2013;19:2366–2379.
18. Boesmans W, Cirillo C, Van den Abbeel V, et al. Neurotransmitters involved in fast excitatory neurotransmission directly activate enteric glial cells. *Neurogastroenterol Motil.* 2013;25:e151–e160.
19. Friedman DJ, Künzli BM, A-Rahim YI, et al. From the Cover: CD39 deletion exacerbates experimental murine colitis and human polymorphisms increase susceptibility to inflammatory bowel disease. *Proc Natl Acad Sci U S A.* 2009;106:16788–16793.
20. Strohmeier GR, Lencer WI, Patapoff TW, et al. Surface expression, polarization, and functional significance of CD73 in human intestinal epithelia. *J Clin Invest.* 1997;99:2588–2601.
21. Louis NA, Robinson AM, MacManus CF, et al. Control of IFN-alphaA by CD73: implications for mucosal inflammation. *J Immunol.* 2008;180: 4246–4255.
22. Deaglio S, Dwyer KM, Gao W, et al. Adenosine generation catalyzed by CD39 and CD73 expressed on regulatory T cells mediates immune suppression. *J Exp Med.* 2007;204:1257–1265.
23. Souza Vdo C, Schlemmer KB, Noal CB, et al. E-NTPDase and E-ADA activities are altered in lymphocytes of patients with indeterminate form of Chagas' disease. *Parasitol Int.* 2012;61:690–696.
24. Gabella G, Trigg P. Size of neurons and glial cells in the enteric ganglia of mice, guinea-pigs, rabbits and sheep. *J Neurocytol.* 1984;13:49–71.
25. Hoff S, Zeller F, von Weyhern CW, et al. Quantitative assessment of glial cells in the human and guinea pig enteric nervous system with an anti-Sox8/9/10 antibody. *J Comp Neurol.* 2008;509:356–371.

26. Panickar KS, Norenberg MD. Astrocytes in cerebral ischemic injury: morphological and general considerations. *Glia*. 2005;50:287–298.
27. Wink MR, Braganhol E, Tamajusuku AS, et al. Nucleoside triphosphate diphosphohydrolase-2 (NTPDase2/CD39L1) is the dominant ectonucleotidase expressed by rat astrocytes. *Neuroscience*. 2006; 138:421–432.
28. Brisevac D, Bajic A, Bjelobaba I, et al. Expression of ecto-nucleoside triphosphate diphosphohydrolase1-3 (NTPDase1-3) by cortical astrocytes after exposure to pro-inflammatory factors in vitro. *J Mol Neurosci.* 2013; 51:871–879.
29. Lavoie EG, Gulbransen BD, Martín-Satué M, et al. Ectonucleotidases in the digestive system: focus on NTPDase3 localization. *Am J Physiol Gastrointest Liver Physiol.* 2011;300:G608–G620.
30. Gulbransen BD, Bashashati M, Hirota SA, et al. Activation of neuronal P2X7 receptor-pannexin-1 mediates death of enteric neurons during colitis. *Nat Med.* 2012;18:600–604.
31. Cavaliere F, Amadio S, Sancesario G, et al. Synaptic P2X7 and oxygen/glucose deprivation in organotypic hippocampal cultures. *J Cereb Blood Flow Metab.* 2004;4:392–398.
32. Morrone FB, Horn AP, Stella J, et al. Increased resistance of glioma cell lines to extracellular ATP cytotoxicity. *J Neurooncol.* 2005;71:135–140.
33. Nasser Y, Keenan CM, Ma AC, et al. Expression of a functional metabotropic glutamate receptor 5 on enteric glia is altered in states of inflammation. *Glia*. 2007;55:859–872.
34. von Boyen GB, Degenkolb N, Hartmann C, et al. The endothelin axis influences enteric glia cell functions. *Med Sci Monit.* 2010;16:BR161: BR167.
35. Voss U, Turesson MF, Robaye B, et al. The enteric nervous system of P2Y13 receptor null mice is resistant against high-fat-diet- and palmitic-acid-induced neuronal loss. *Purinergic Signal.* 2014;10:455–464.
36. Bennett MV, Garré JM, Orellana JA, et al. Connexin and pannexin hemichannels in inflammatory responses of glia and neurons. *Brain Res.* 2012; 1487:3–15.
37. Christofi FL. Unlocking mysteries of gut sensory transmission: is adenosine the key? *News Physiol Sci.* 2001;16:201–207.
38. Cirillo C, Sarnelli G, Turco F, et al. Proinflammatory stimuli activates human-derived enteroglial cells and induces autocrine nitric oxide production. *Neurogastroenterol Motil.* 2011;23:e372–e382.
39. MacEachern SJ, Patel BA, Keenan CM, et al. Inhibiting inducible nitric oxide synthase in enteric glia restores electrogenic ion transport in mice with colitis. *Gastroenterology*. 2015;149:445–455.e3.
40. Gulbransen BD, Sharkey KA. Purinergic neuron-to-glia signaling in the enteric nervous system. *Gastroenterology*. 2009;136:1349–1358.
41. Sofroniew MV. Astrocyte barriers to neurotoxic inflammation. *Nat Rev Neurosci.* 2015;16:249–263.
42. Lopes JE, Torgerson TR, Schubert LA, et al. Analysis of FOXP3 reveals multiple domains required for its function as a transcriptional repressor. *J Immunol.* 2006;177:3133–3142.
43. Jack CS, Arbour N, Manusow J, et al. TLR signaling tailors innate immune responses in human microglia and astrocytes. *J Immunol.* 2005;175:4320–4330.
44. Sugimoto K, Ogawa A, Mizoguchi E, et al. IL-22 ameliorates intestinal inflammation in a mouse model of ulcerative colitis. *J Clin Invest.* 2008; 118:534–544.
45. Zindl CL, Lai JF, Lee YK, et al. IL-22-producing neutrophils contribute to antimicrobial defense and restitution of colonic epithelial integrity during colitis. *Proc Natl Acad Sci U S A.* 2013;110:12768–12773.
46. Schultz M, Lai CC, Lindstroem AL, et al. Aggravation of established colitis in specific pathogen-free IL-10 knockout mice by restraint stress is not mediated by increased colonic permeability. *J Crohns Colitis*. 2015; 9:754–762.
47. Mannon PJ, Fuss IJ, Mayer L, et al. Anti-interleukin-12 antibody for active Crohn's disease. *N Engl J Med.* 2004;351:2069–2079.
48. Sandborn WJ, Gasink C, Gao LL, et al. Ustekinumab induction and maintenance therapy in refractory Crohn's disease. *N Engl J Med.* 2012;367:1519–1528.
49. Rolhion N, Darfeuille-Michaud A. Adherent-invasive Escherichia coli in inflammatory bowel disease. *Inflamm Bowel Dis.* 2007;13:1277–1283.
50. Brun P, Giron MC, Qesari M, et al. Toll-like receptor 2 regulates intestinal inflammation by controlling integrity of the enteric nervous system. *Gastroenterology*. 2013;145:1323–1333.
51. Murakami M, Ohta T, Ito S. Lipopolysaccharides enhance the action of bradykinin in enteric neurons via secretion of interleukin-1beta from enteric glial cells. *J Neurosci Res.* 2009;87:2095–2104.
52. Neunlist M, Rolli-Derkinderen M, Latorre R, et al. Enteric glial cells: recent developments and future directions. *Gastroenterology*. 2014;147: 1230–1237.
53. Bradley JS Jr, Parr EJ, Sharkey KA. Effects of inflammation on cell proliferation in the myenteric plexus of the guinea-pig ileum. *Cell Tissue Res.* 1997;289:455–461.
54. Neurath MF. Cytokines in inflammatory bowel disease. *Nat Rev Immunol.* 2014;14:329–342.
55. Abdo H, Derkinderen P, Gomes P, et al. Enteric glial cells protect neurons from oxidative stress in part via reduced glutathione. *FASEB J.* 2010;24: 1082–1094.
56. Anitha M, Gondha C, Sutliff R, et al. GDNF rescues hyperglycemia-induced diabetic enteric neuropathy through activation of the PI3K/Akt pathway. *J Clin Invest.* 2006;116:344–356.
57. Cheng Y, Takeuchi H, Sonobe Y, et al. Sirtuin 1 attenuates oxidative stress via upregulation of superoxide dismutase 2 and catalase in astrocytes. *J Neuroimmunol*. 2014;269:38–43.
58. Schreiner B, Romanelli E, Liberski P, et al. Astrocyte depletion impairs redox homeostasis and triggers neuronal loss in the adult CNS. *Cell Rep*. 2015;12:1377–1384.
59. Desagher S, Glowinski J, Premont J. Astrocytes protect neurons from hydrogen peroxide toxicity. *J Neurosci.* 1996;16:2553–2562.
60. Retamal MA, Alcayaga J, Verdugo CA, et al. Opening of pannexin- and connexin-based channels increases the excitability of nodose ganglion sensory neurons. *Front Cell Neurosci*. 2014;8:158.
61. Lin SH, Song W, Cressatti M, et al. Heme oxygenase-1 modulates microRNA expression in cultured astroglia: implications for chronic brain disorders. *Glia*. 2015;63:1270–1284.
62. Aubé AC, Cabarrocas J, Bauer J, et al. Changes in enteric neurone phenotype and intestinal functions in a transgenic mouse model of enteric glia disruption. *Gut*. 2006;55:630–637.
63. Zamanian JL, Xu L, Foo LC, et al. Genomic analysis of reactive astrogliosis. *J Neurosci.* 2012;32:6391–6410.
64. Silva-García O, Valdez-Alarcón JJ, Baizabal-Aguirre VM. The Wnt/β-catenin signaling pathway controls the inflammatory response in infections caused by pathogenic bacteria. *Mediators Inflamm.* 2014;2014:310183.
65. Rao M, Nelms BD, Dong L, et al. Enteric glia express proteolipid protein 1 and are a transcriptionally unique population of glia in the mammalian nervous system. *Glia*. 2016;63:2040–2057.